Studies of cosmic ray showers using neon flash tubes

Scull, P. S.

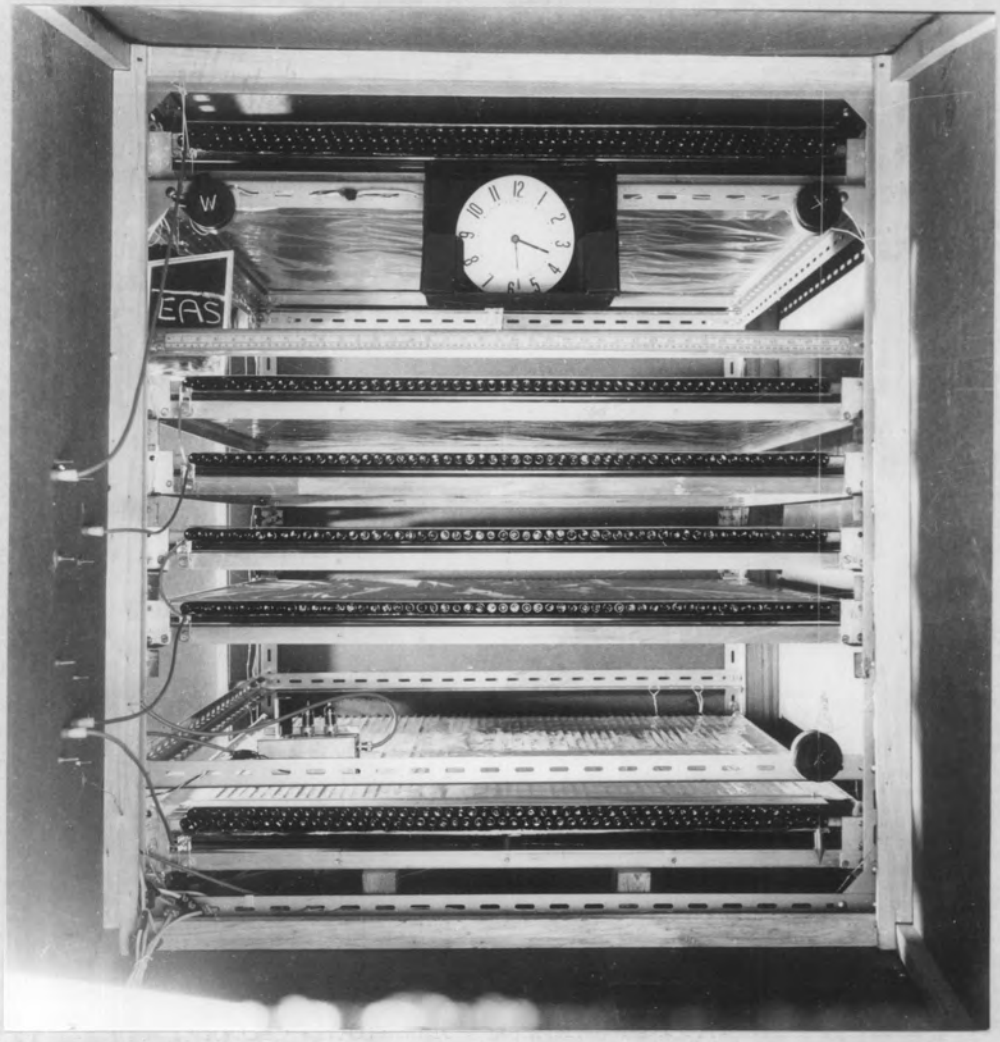

The Directional Air Shower Indicator

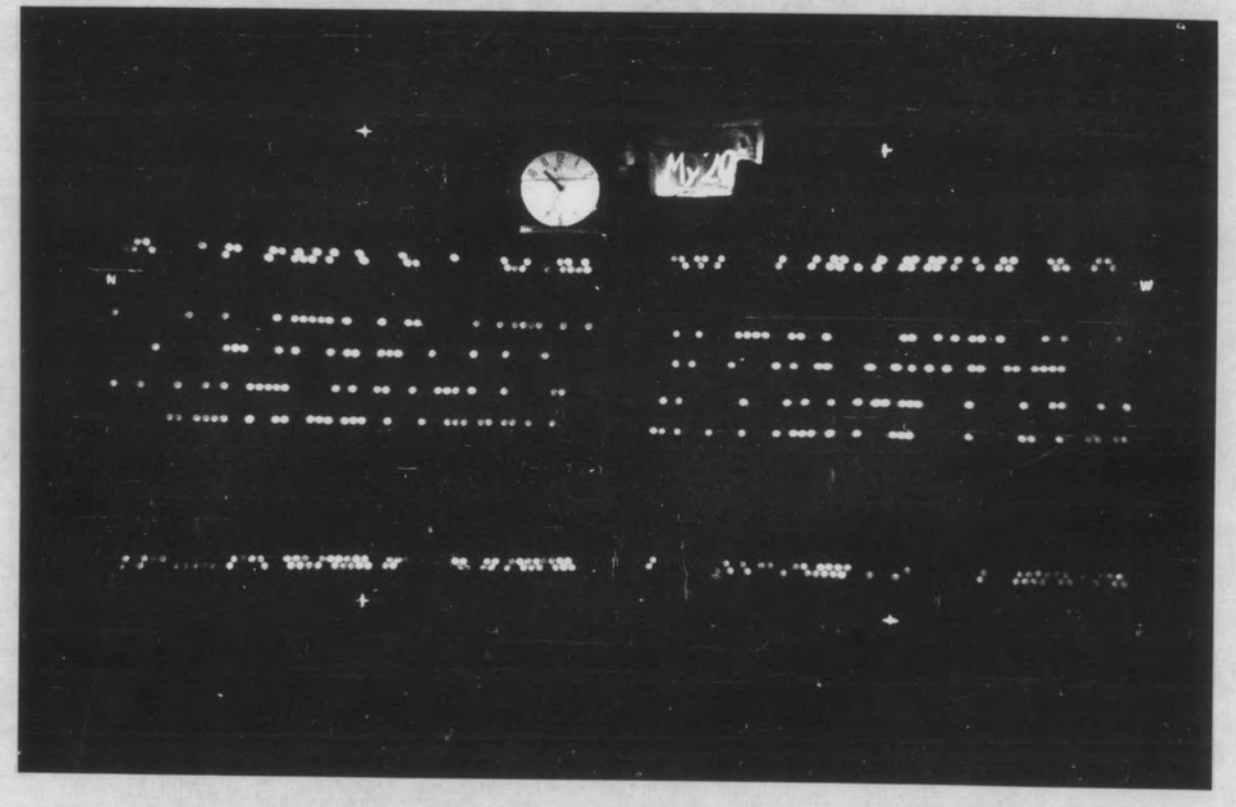

A typical event used in the determination of the density spectrum. Obtained using D.A.S.I. as modified for the Silwood Experiment

Studies of Cosmic Ray Showers using Neon Flash Tubes

A Thesis presented by

P. S. Scull

for the degree of Master of Science

at

The University of Durham

July
1962

Contents

Abstract

This thesis describes experiments to determine the properties of the light output from neon flash-tubes traversed by ionizing particles under a wide range of conditions together with the determination of the density spectrum of extensive air showers in the region of mean shower size $\overline{N} = 9 \times 10^5$ particles.

It is shown that the intensity of the light output of the flash-tube in an array is such that an accurate estimate of the number of flashed tubes may be made by determining the total amount of light emitted using a photomultiplier. The possibilities of using this technique are discussed.

Extensive air showers were selected by an array of four Cerenkov detectors and the particle density at a large flash-tube array was obtained for each shower. The slope of the differential density spectrum was found to be -3.3 ± 0.3. Comparisons were carried out between the expected shower sizes obtained by the Cerenkov detectors and the flash-tube array for different ranges of density and distances from the shower core. A calibration of the Cerenkov detectors was obtained. The relationship between these results and those of other workers are considered.

Preface

The work described in this thesis was carried out during the author's tenure of a D.S.I.R. Advanced Course Studentship at the Durham Colleges in the University of Durham. The work was performed under the supervision of Dr. A.W. Wolfendale.

The optical measurements were made by the author and the results were interpreted by the author and his colleagues. This work has been published by the author and Drs. Coxell, Meyer and Wolfendale (1962).

Measurements of the density of particles in extensive air showers were made using apparatus designed by Dr. Coxell and the apparatus was operated jointly by the author and Dr. Coxell. The analysis of the results was the sole responsibility of the author.

LIST OF FIGURES

Chapter 1

Introduction

The study of Cosmic Rays has been the subject of intensive research since their discovery at the beginning of the present Century. The radiation has been shown to consist of atomic particles, having a very wide spectrum of energies and comprising particles of a variety of masses, and γ-rays. Information on the nature of the radiation has been obtained by many different methods, ranging from the use of rocket-borne instruments above the earth's atmosphere, to observations with detectors far underground. The study of the cosmic radiation has led to the discovery of several elementary particles and has improved our knowledge of the nuclear processes which occur; it has also stimulated the development of numerous instruments for the observation of ionizing particles.

It is now possible to study nuclear interactions under laboratory conditions using particle accelerators such as the proton synchrotron at C.E.R.N. The highest energy achieved, 30 GeV, is however, low by cosmic ray standards and for particles of higher energy we must resort to the cosmic radiation.

The earth's atmosphere is under the continuous bombardment of high energy particles coming from outer space and these constitute the primary component of the

radiation. As they penetrate into the atmosphere these particles lose energy by ionizing collisions and eventually collide with nuclei of nitrogen and oxygen. The collisions mainly occur at heights above sixteen kilometres, and result in the production of a secondary radiation consisting of particles of lower energy and different nature.

The primary cosmic radiation consists of approximately eighty-five per cent. protons, fifteen per cent. α-particles and a small fraction of heavier nuclei with atomic numbers up to twenty-six. In the collisions which occur in the atmosphere secondary protons, neutrons, charged and neutral π-mesons and hyperons are produced. Few of these survive to sea level, however. The decay of the neutral π-mesons into pairs of photons, through the complementary processes of pair creation and bremsstrahlung, leads to the formation of a large number of electron-photon cascades. Charged π-mesons behave differently, decaying into μ-mesons and neutrinos. μ-mesons have a very weak interaction with matter and thus lose energy in their passage towards the earth almost entirely by ionization alone. The μ-meson is also unstable, decaying into an electron and two neutrinos. Thus the radiation observed at sea level consists mainly of protons, neutrons, π-mesons, μ-mesons, electrons, photons and neutrinos. As the μ-mesons do not undergo radiation

losses comparable to those of electrons, and do not suffer nuclear collisions as do protons and neutrons, they become relatively more abundant through the atmosphere and at sea level compose roughly half of the observed radiation.

When a primary particle of very high energy ($\gtrsim 10^{16}$ eV) enters the earth's atmosphere it starts a chain of interactions giving rise to millions of secondary particles having a lateral spread at sea level of hundreds of metres. This phenomenon is known as an Extensive Air Shower (E.A.S.). The properties of E.A.S. will be discussed more fully in the following chapters.

In common with most other branches of science, advances have followed improvements in technique. Early studies of cosmic rays were carried out with ionization chambers which were used to measure the total amount of ionization produced within the chamber. These studies showed how the radiation varied with altitude and from place to place over the earth's surface. With the development of the Cloud Chamber and the Geiger-Müller counter in the 1920's, studies of the behaviour of individual particles became possible, and advances were made in our understanding of nuclear physics. For example, two new fundamental particles were discovered in the cosmic radiation; the positron and the μ-meson. Similar advances came in the 1940's from the introduction of the nuclear emulsion.

Recent years have seen the increasing use of scintillation and Cerenkov counters, a development due mainly to the introduction of efficient photomultipliers. These detectors have the advantage of a high speed of response, and they are comparatively simple to operate.

A technique of very recent introduction, and one which has been used in the investigations reported in this thesis, is the neon flash-tube. This is another technique of essential simplicity and one that is finding increasing application in cosmic ray studies.

This thesis will deal with the use of the neon flash-tube, as developed in Durham, in an array to study the density spectrum of Extensive Air Showers. Chapter 2 provides a summary of the properties of Extensive Air Showers. Chapter 3 describes investigations on the optical properties of the flash-tube and Chapters 4, 5 and 6 give an account of the properties of the flash-tube array and its application in specific experiments.

Chapter 2

Extensive Air Showers

2.1 Introduction

In an extensive air shower the secondary particles caused by many interactions arrive at sea level at practically the same time over a plane perpendicular to the direction of the original particle. They are distributed around the direction of the original particle, known as the axis of the shower, out to great distances. No method has yet been found to observe the very high energy primaries directly, due to their low intensity. The frequency of arrival of a primary cosmic ray of energy $>10^{16}$ eV over an area of 1 sq. metre is about one per month and for a particle of energy $>10^{18}$ eV roughly one in 3000 years. The low density of the atmosphere permits the secondaries to spread out sufficiently for detectors to resolve and count them. The vertical thickness of the atmosphere is such that it allows almost all showers to develop fully and by determining the number of particles present at the level of observation the total energy may be obtained. The great number of secondaries which form the air shower allows us to detect the energetic primary particles incident on the earth's atmosphere with relatively high frequency. With a suitable array of detectors, showers of $>10^{17}$ eV may be detected at a rate of one per day at sea

level. The study of the primary particle is therefore indirect, and its properties can only be arrived at by careful analysis of the secondary particles.

The density spectrum of showers, i.e., the frequency of showers having particle densities at a recording device greater than a given value, yields information on the development process of the shower. Similar information comes from the measurement of the frequency-size or frequency-number spectrum, and from this spectrum it is possible to determine the energy spectrum of the primary particles if assumptions are made about the cascade process. It has been shown that this may be done with reasonable accuracy by assuming that the shower is simply an electron-photon cascade.

Early results of measurements on air showers near sea level indicated that the showers consisted of electrons and photons. Later measurements showed the additional existence of a penetrating component composed of μ-mesons and nucleons. Because electrons are by far the most numerous particles near the axis of a large shower, they are the easiest to detect. Thus, although interest may centre on the nucleonic cascade of which the electronic component is the outgrowth, it is necessary first to understand the development of the electronic component.

2.2 The Lateral Structure of Extensive Air Showers

One of the most frequent parameters to be measured of E.A.S. is the average lateral distribution of the total charged particle density. It should be noted here that it is only with the advent of large and complex detecting arrays, as have been used in America, Japan and Russia, that it is possible for accurate distributions of particles to be obtained for individual showers. The form of the average distribution is found to agree with that obtained for a pure electromagnetic cascade, in which the lateral distribution is entirely due to the Coulomb scattering of electrons.

According to the cascade theory, the local density of electrons can be written as

$$\Delta(r) = \frac{N}{r_1^2} f(r)_s \qquad 2.1$$

where N is the total number of electrons at the level of observation, r_1 is the Moliere unit and $f(r)_s$ is the structure function independent of N but varying with the age of the shower. The age of the shower is reflected in an age parameter s. For showers measured at sea level the value of r_1 is 79 metres.

Greisen (1960) has obtained an empirical analytic function for a shower of 10^6 charged particles at sea level which takes the form

$$\Delta(N,r) = \frac{0.4N}{r_1^2}\left(\frac{r_1}{r}\right)^{0.75}\left(\frac{r_1}{r+r_1}\right)^{3.25}\left(1+\frac{r}{11.4r_1}\right) \qquad 2.2$$

Omitting the last factor on the right hand side, equation 2.2 is a close approximation to the theoretical function derived by Nishimura and Kamata (1958) for an electromagnetic cascade having an age parameter of s = 1.25. This function has been found to hold for showers of size 2.10^3 to 2.10^9 charged particles.

Fukui et al.(1960) have found the following relation for the lateral distribution, in a range from several metres to two hundred metres from the axis:

$$\Delta(r) \propto \frac{1}{r^{1.5}} \cdot \exp\left(-\frac{r}{120}\right) \qquad 2.3$$

and that if this shape is to be represented by the Nishimura and Kamata function, s must have a value of 0.6 - 0.8 for r = 3-30m, and 1.2 - 1.4 for r≥30m. This is somewhat different from the value of s = 1.25 quoted by Greisen for the range 5 cm to 1500 m. Whilst Fukui et al found that the distribution for r<3m fluctuates from shower to shower they stated that this is only a tentative result.

By the use of detectors measuring the energy flow of the electron component, the lateral distribution of energy flux may be obtained with the prior knowledge of the position of the shower axis. It has been found that the shape of the energy distribution is independent of the size of the showers and also of the elevation at which they

are detected. The slope of the distribution is found to increase with increasing distance from the shower axis, the showers being poorer in high energy electrons and photons at large radii. After having obtained the average energy per particle as a function of distance from the shower axis, the total energy carried by the electron-photon component may be estimated by integrating the energy flow over the whole shower. The result is 0.2N GeV, where N is the total number of electrons in the shower.

2.3 The Lateral Distribution of μ-mesons

Assuming that the lateral distribution of μ-mesons is independent of the total number of charged particles, N, Clark et al.(1958) have obtained a function which is similar to equation 2.2.

$$\Delta_{\mu}(N,r) = 18 \left(\frac{N}{10^6}\right)^{\frac{3}{4}} r^{-\frac{3}{4}} \left(1 + \frac{r}{320}\right)^{-2.5} \qquad 2.4$$

The lateral distribution is dependent on the minimum energy required for the detection of mesons, and for the results quoted energies exceeding 1 GeV were required. Near the axis, experiments have shown the distribution to be proportional to $r^{-\frac{3}{4}}$, also, it appears that the number of μ-mesons is not proportional to the shower size but to $N^{\frac{3}{4}}$.

Fukui et al.(1960) have found that the total number of μ-mesons in each shower of the same size fluctuates widely. The fluctuation has been attributed to fluctua-

tions in the point of the first interaction of the E.A.S. in the atmosphere.

2.4 The Lateral Distribution of the Nuclear-active Component

In an E.A.S., particles of very high energy are found closer to the shower axis than those of lower energy, as would be expected. No particles of the nuclear-active component of energy above 10^{11} eV have been observed at distances greater than 40 metres. It has been shown, by detailed studies of the shower core with a diffusion chamber, that the particle density distribution has a radial dependence of r^{-n} with

$$n = 0.6 \pm 0.1 \text{ for } 5 \text{ cm} < r < 30 \text{ cm}$$

$$n = 1.0 \pm 0.1 \text{ for } 30 \text{ cm} < r < 3\text{m}.$$

For a range of $1\text{m} < r < 30\text{m}$ a value of $n = 2.0 \pm 0.2$ has been quoted. This seems to emphasise the intense angular collimation exhibited by the N-component and suggests that the radius of the shower core is in the region of 30 cm. A large part of the total energy is carried by a few particles and fluctuations in the lateral distribution of particles near the shower axis are not entirely unexpected.

2.5 The Longitudinal Development of Extensive Air Showers

It is not possible to obtain direct information on the development of a shower but this may be inferred from measurements of the shower-size spectrum and from the dependence of shower rate on altitude. The rate at which showers of size N_s are observed at sea level is given by

the integral size spectrum

$$K(N_s) \propto N_s^{-\gamma} \qquad 2.5$$

A shower at depth t, of size N_s at sea level, has size N given by

$$N = RN_s\, e^{-t/\lambda} \qquad 2.6$$

where R is a constant and λ is the attenuation length. From electron-photon cascade theory it can be shown that the number of particles in a shower decreases exponentially beyond the maximum.

Considering showers of the same size, the rate of occurrence at depth t is,

$$(N_s)^{-\gamma} = \left[\frac{1}{R} N_o e^{+t/\lambda}\right]^{-\gamma} \propto \left(\frac{N}{R}\right)^{-\gamma} e^{-\gamma t/\lambda} \qquad 2.7$$

Thus, by observing showers of constant size and measuring the variation of rate with depth, we can obtain the absorption factor $e^{-t/\Lambda}$, where $\Lambda = \lambda/\gamma$ is the absorption length of the shower.

A useful method of obtaining the absorption length is to study the variation of shower rate with inclination to the vertical, i.e. the zenith angle distribution. If $s(N,x)$ is the differential number spectrum of showers, per unit area per unit time per unit solid angle, having N particles at atmospheric thickness x, then

$$s(N,x) \propto \exp -\left(\frac{x-x_o}{\Lambda}\right) \qquad 2.8$$

where x_o is the vertical depth of the atmosphere. At a

zenith angle θ, the atmospheric thickness will be increased to

$$x = x_0 \sec \theta$$

thus,

$$s(N,\theta) \propto \exp -\left(\frac{x_0}{\Lambda} (\sec \theta - 1) \right)$$

$$\propto 1 - \frac{x_0}{\Lambda} \cdot \frac{\theta^2}{2} \qquad 2.9$$

It is found experimentally, to quite high accuracy, that

$$s(N,\theta) \propto \cos^n \theta$$

that is,

$$\propto 1 - n \frac{\theta^2}{2} \qquad 2.10$$

comparing equation 2.9 and 2.10 we obtain

$$n = \frac{x_0}{\Lambda} \qquad 2.11$$

Thus, Λ the absorption length may be obtained from an experimental determination of n. The expression relating Λ to λ, the attenuation length,

$$\lambda = \gamma \Lambda \qquad 2.12$$

where γ is the slope of the density spectrum, is only true if the shower starts its development essentially at a fixed place. Current determinations show that λ has a value in the range 200 to 250 gm.cm^{-2}. This is, however, a complicated average of the absorption length over some showers that are still growing and others that are dying out. A further complication is that fluctuations in the development occur and a satisfactory method of allowing for their effect does not appear to have been made.

The conclusion that can be drawn from this discussion of selected topics is that it is highly desirable to study as many aspects of showers as possible and to use a variety of experimental techniques. With this object in view the possibility of using the recently developed flash-tube technique was examined, and a flash-tube array was operated at Durham and later at Silwood Park. Before describing the array the results will be given of some investigations on the flash-tube technique, with particular reference to measurements on the properties of the flash of light emitted by a tube.

Chapter 3

Optical Measurements on Neon Flash-Tubes

3.1 Introduction

The flash of light emitted by the tube when a high voltage pulse is applied across it, is the colour of the predominant spectral lines of neon, namely, bright red. The properties of this flash, its intensity and duration, have been studied with the possibility of further applications of the tube in an array such as the Directional Air Shower Indicator where a photomultiplier could be used as an integrating device to give an output pulse accurately proportional to the number of flash-tubes "discharged". The measurements were therefore divided into two main groups; those dealing with the properties of single tubes and those concerned with the properties of an array of tubes. To a certain extent the properties of an array can be inferred from measurements on single tubes, but certain differences peculiar to arrays have been obtained. These differences are important when one is considering a large array and will be discussed in detail.

3.2 The Experimental Arrangement

The tubes used in the measurements were constructed from soda glass tubing of internal diameter 1.5 cm, wall thickness 1 mm, and were of two lengths, 27 cm and 115 cm.

Commercial Neon at a pressure of 65 cm Hg was used as filling. These tubes have been developed specially for use in extensive air shower experiments and more general properties will be given in the next chapter. The photomultiplier system consisted of an E.M.I. photomultiplier, Type 6095, followed by a cathode follower. The pulses were applied to a Solartron Oscilloscope (Types CD643.S or 513.2) and their heights recorded both visually and in the case of the array of tubes, photographically.

To provide the initiating ionization in the case of measurements on single tubes a radioactive source (10mc ^{60}Co) was used. Cosmic rays, selected by a four-fold Geiger telescope consisting of a pair of crossed counters above the array and a pair below, were used for measurements on the array of 25 tubes.

The high voltage pulsing system has been described previously (Coxell et al., 1960), where for most of the work the pulse applied to the plates was derived from a circuit in which a single condenser was discharged through a trigatron and the resulting pulse amplified by a pulse transformer. The magnitude of the pulse was varied by varying the tapping on an impedance chain connected across the output of the pulse transformer.

An accurate calibration curve was determined for the photomultiplier system by various standard procedures thus allowing measurements to be carried out in the linear region of the system.

3.3 Characteristics of Single Tubes

The following factors have been investigated.

1. The position along the length of the tube of the ionizing particle trajectory.
2. The variation of light output with magnitude of the high voltage pulse.
3. The angle with respect to the axis of the tube at which the intensity is measured.
4. The variation of intensity from one tube to another.
5. The variation of light output for one tube from one pulse to the next.

3.3.1 The Position of the Ionizing Particle

Studies were made of the discharge using a radioactive source at different positions along the length of the tube. A variation was found in the intensity such that the intensity was higher when the source was placed at the far end of a 115 cm tube. This variation amounted to 22% from one end of the tube to the other. This result indicates that the discharge is brighter in the region of the source and also the possibility of an improvement in intensity due to internal reflections along the tube. It is of note that no difference in intensity along an unpainted tube was observed visually when the tube was discharged in a darkened room. Coxell et al.(1961), operating an array of tubes to define the particle trajectory together with unpainted tubes at right angles to the array, obtained

photographs of the discharge. It was shown that the discharge took the form of streamers occupying the length of the tube between the electrodes and also that there were no apparently brighter streamers where the particle passed through the tubes. This is contrary to observations made by Fukui and Miyamoto (private communication) where a distinctly bright discharge column was seen. No definite conclusion can be drawn to explain this discrepancy, although differences in pulse characteristics may have an effect.

Unfortunately, the variation in intensity is too small to be of practical use to denote the position of the trajectory with any accuracy. In all subsequent experiments, however, the source was placed in a standard position to obviate any uncertainty in the results.

3.3.2 The Variation from One Pulse to the Next

In this investigation forty-five of the 115 cm tubes were each subjected to fifty pulses with an interval of about two seconds between each pulse. This ensured that the power supplies for the trigatron had recovered fully from the previous discharge and that the discharging condenser was fully charged to 8 kv. The pulse heights from the photomultiplier were noted and the differences from the mean for each tube were obtained. All the differences were combined to give the distribution in figure 3.1.

When corrections for the error in measuring the pulse heights have been made the standard deviation (σ_1) of a

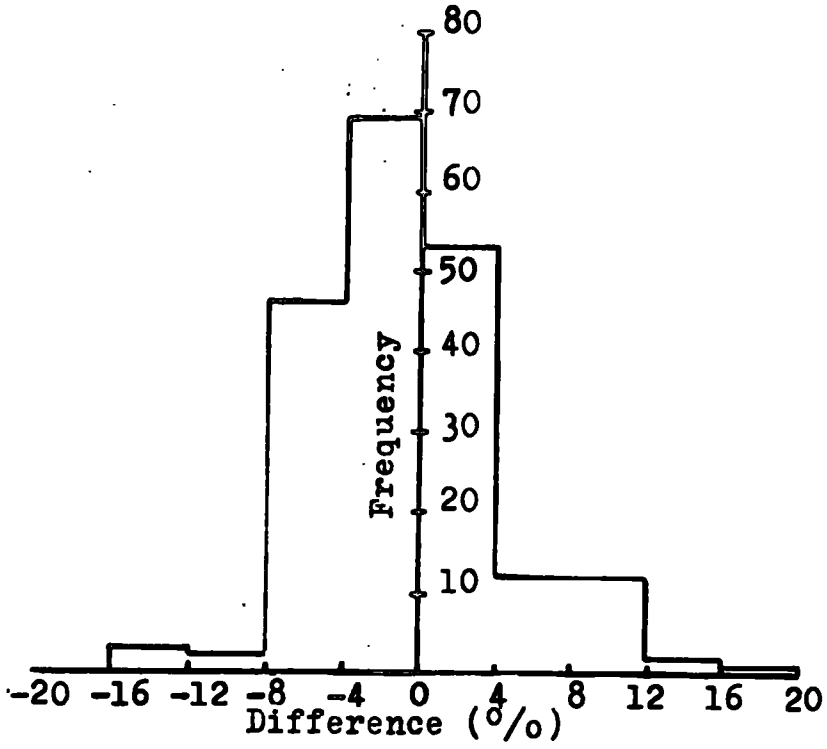

Fig.3.1. The Variation in Pulse Height about the Mean.

single reading from the mean is found to be 5.1%. If effects such as variations in the gain of the photomultiplier, oscilloscope and amplifiers were taken into account the value of σ_1 would be still less.

It is therefore possible to conclude that, due to this small variation in light output from one pulse to the next, the discharge mechanism is essentially reproducible and that quantitative measurements should be possible.

3.3.3 The Variation of Light Intensity from One Tube to the Next

As in the previous investigation forty-five tubes were used. Several batches, each of 5 or 10 tubes, were selected from over 900 tubes, each batch representing a different filling, as groups of tubes (usually 60) were filled at the same time on a high vacuum system. The purpose of this investigation was to show whether a large variation in light output could be observed from batch to batch despite the fact that the filling may be to the same pressure. Also, variations are to be expected from differences in the 'end-window' of the tube, which arise during the construction of the tube, affecting the amount of light emerging from it. The results of the investigation are shown in figure 3.2.

The resulting standard deviation (σ_2) for all the tubes from the overall mean is calculated to be 17%. From figure 3.2 it is evident that there is a significant varia-

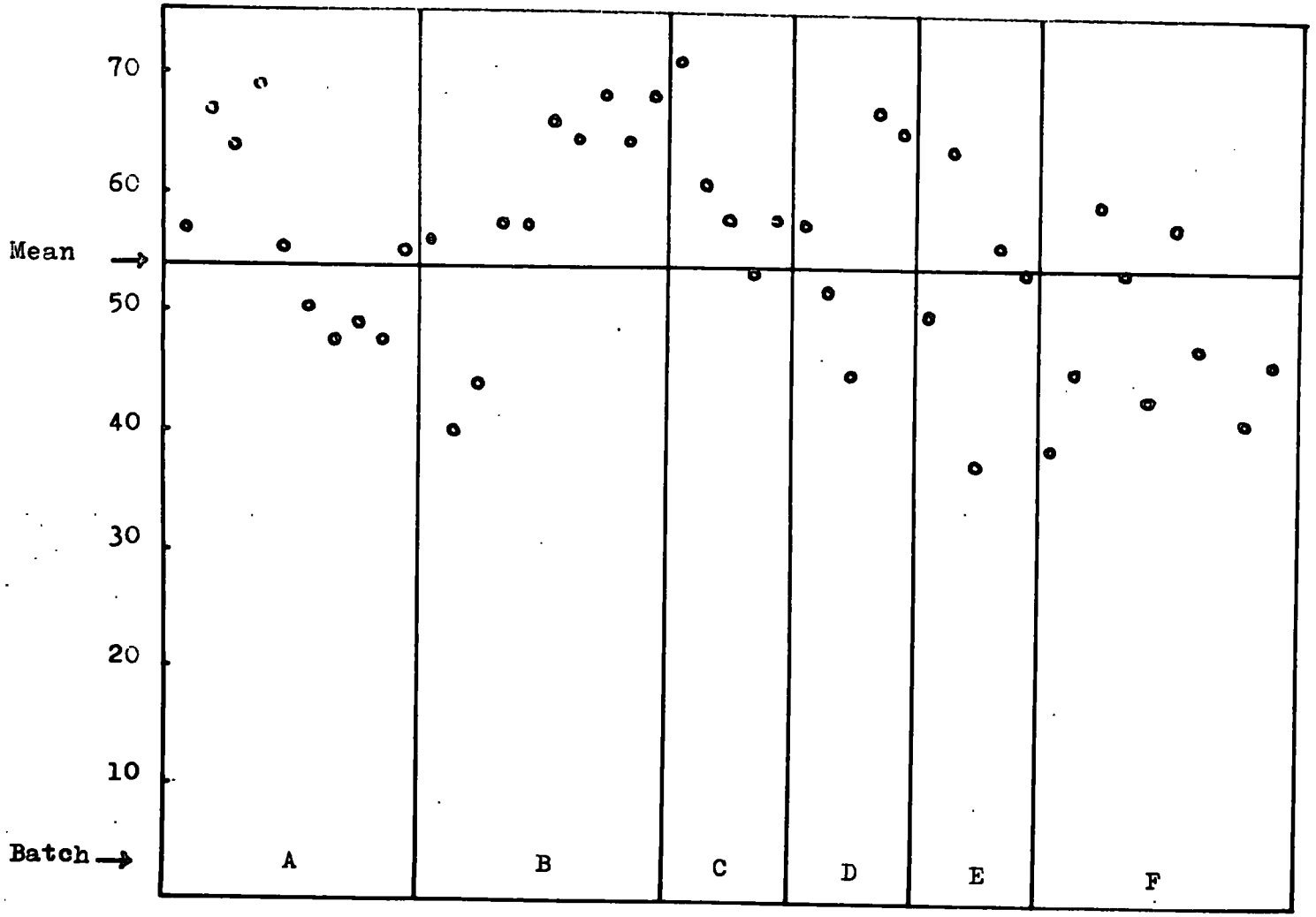

Fig.3.2. The variation of intensity from tube to tube.

tion between batches as well as a variation within each batch. For most applications σ_2 is not too large and could possibly be reduced by using greater care in the glass blowing of the tubes and the filling technique. Another possibility is to sort the tubes into batches having different mean values, and adjust the applied field accordingly to give a constant light output for each batch (layer) in an array.

3.3.4 The Polar Diagram

When a photomultiplier is used to measure the light output from an array of tubes it records light from tubes which necessarily make different angles with the photomultiplier tube axis. Measurements were made of the polar diagram in the plane perpendicular to the direction of the field (horizontal plane) for both short and long tubes with the results shown in figures 3.3. and 3.4. The geometrical arrangement being shown in the inset of figure 3.4. The separation of the tube and the photomultiplier, d, was made sufficiently great for the smearing of the distribution, due to the finite angle subtended by the photocathode, to be small. In the case of the long tubes d was 425 cm.

A rapid fall-off of intensity was found, especially for the long tube. A rather less rapid fall-off was found in the vertical plane, probably due to the form of the dis-

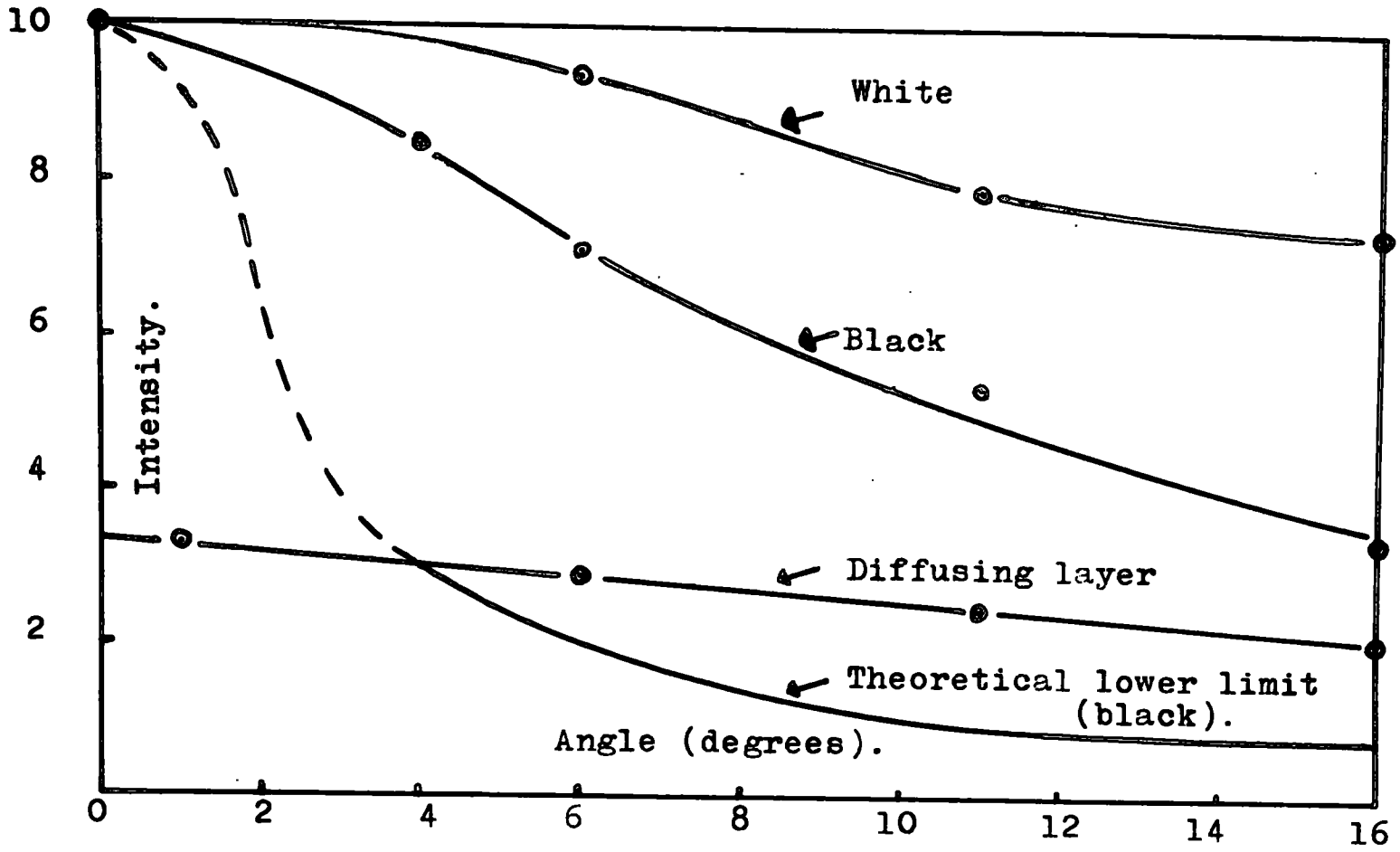

Fig.3.3. Polar diagram for short tube.

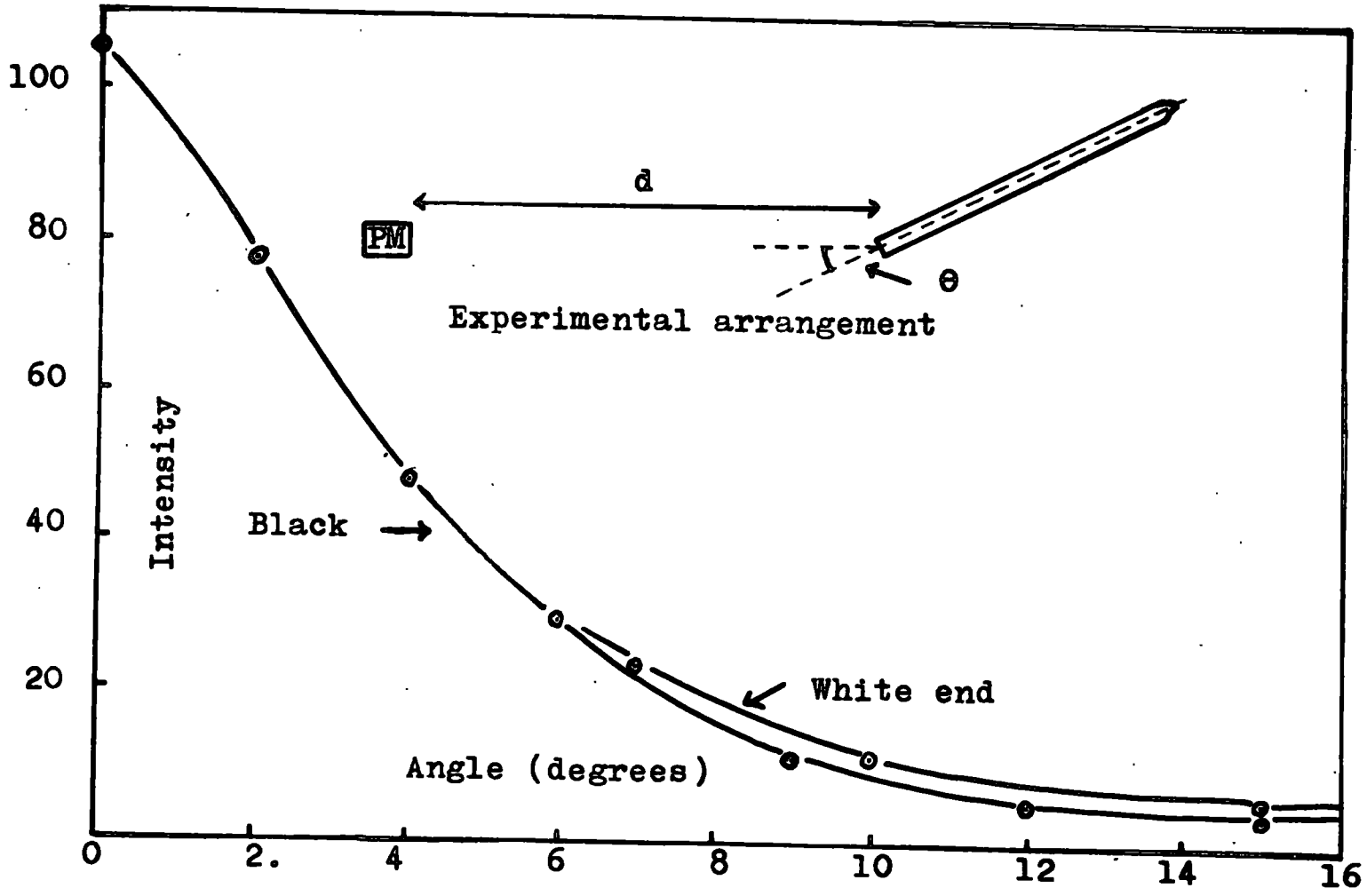

Fig.3.4. Polar diagram for the long tube.

charge appearing as vertical streamers which have a less marked variation in the vertical plane.

Included in figure 3.3 is a curve showing a theoretical variation in intensity with angle. This has been calculated by making the following assumptions:

1. Reflections and self-absorption are unimportant.
2. A uniform cylinder of emitting gas, i.e. neglecting the filamentary nature of the discharge.

If V_o is the volume of the cylinder and V_θ is the volume which is observed at angle θ through the circular end window, then the variation in intensity is given by,

$$\frac{I_o}{I_\theta} = \frac{V_o}{V_\theta}$$

If the internal diameter of the tube is 2r and the length of the tube between the electrodes is $2\underline{l}$, then, if the end window of the tube is flush with the end of the electrodes, it can be shown that

$$\frac{V_\theta}{V_o} = \frac{4}{3\pi} \cdot \frac{r}{\underline{l}} \cot \theta \qquad \text{for } \theta > \theta_o, \text{ where } \tan \theta_o = \frac{r}{\underline{l}}$$

(see appendix I).

It is immediately noticeable that the observed variations show much greater intensities than does the theoretical curve. The most likely reason for this is that reflections play a prominent role in increasing the intensity.

A short tube which was painted white over its entire length was found to give a less steep variation with increasing angle than the black tubes. Accordingly, the longer tubes were scraped of their black paint for 20 cm and this length was then painted white with an overcoat of black paint. This black overcoat decreases the probability of a tube firing its neighbour when it discharges. The result is shown in figure 3.4. The improvement obtained by the use of white paint amounts to 50% at $\theta = 12^{\circ}$ and is encouraging for the photography of arrays. All the tubes in the extensive air shower array, to be described later, were stripped and repainted in the above manner. A noticeable improvement in the photographic recording was observed. Unfortunately, the improvement is not sufficient for use with a photomultiplier looking directly at the array at angles of the order of $\theta = 10^{\circ}$ as the peaking of the polar diagram for the white-ended tubes is still too sharp. This sharp peaking could be reduced by the use of a diffusing surface on the end window of the tube. Although there is a reduction in absolute intensity it is seen in figure 3.4 that the variation is much less steep. The absolute value is not important in photomultiplier measurements.

3.3.5 The Variation of Light Output with Field Strength

Figure 3.5 shows the variation obtained by varying the pulse height applied to the electrodes. The tube was placed in a fixed position at $\theta = 0^{\circ}$ for these observations. The

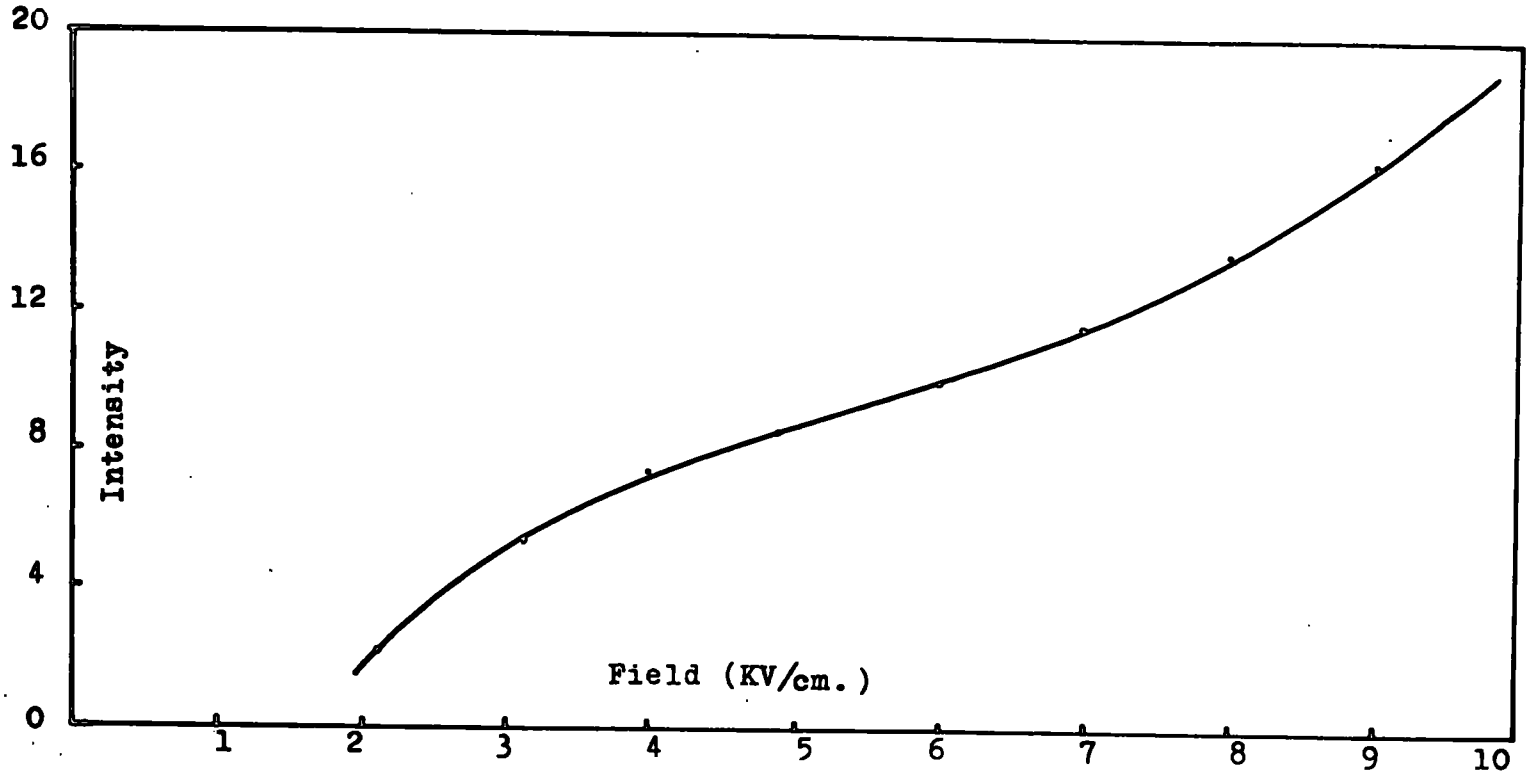

Fig. 3.5. Variation of intensity with field strength.

curve given is for the long tube whilst a very similar curve can be obtained for the short tube.

A parallel may be drawn at low field strengths between the pulse height in a Geiger counter and the variation in light output of the flash-tube. However, above field strengths of 6 kv/cm the rate of rise of the flash-tube light pulse increases whereas in the case of the Geiger counter a falling rate of rise is exhibited.

3.4 Characteristics of an Array of Long Tubes

The studies of the optical properties of single tubes have given information on the reliability of the tube. What is now most important is the possibility of using the photomultiplier for the selection of particular events. Interest could then be placed in events where only a certain number of tubes were discharged. This has importance in the field of extensive air showers where, if the light output is directly related to the number of tubes discharged, the density spectrum of showers could be obtained by recording the pulse heights on a pulse height analyser. This would save the long periods of time spent in the analysis of film records of showers where the number of tubes which have flashed have to be counted. The photomultiplier may also be used as a selector of events in conjunction with a camera having a shutter and making use of the 'After-flashing' characteristics of the flash-tube (Coxell et al.,1961).

3.4.1 Variation of Integrated Intensity with the Number of Discharged Tubes

The array consisted of 25 long tubes, - five layers of 5 tubes in each, between electrodes of length 25 cm. A simple Geiger counter system to select cosmic rays provided the triggering pulses. The flashes were photographed directly and at the same time the pulse heights from the photomultiplier were photographed on the oscilloscope. It was therefore possible to correlate the pulse height obtained with the number of tubes which have flashed. Figure 3.6 curve (a) shows that there is departure from linearity after more than four tubes have been discharged, and that there is a reduction in the rate of increase of pulse height with the number flashed. This result can be attributed to the finite output impedance of the electronic circuit providing the high voltage pulse and hence the lack of proportionality. Also, the small rate of rise obtained together with the fluctuations observed in the investigations on the characteristics of single tubes means that the accuracy which can be expected by a single pulse from the photomultiplier will be low.

The output impedance of the pulse generator was reduced by dispensing with the pulse transformer and by using a low terminating impedance. The results are shown as curves(b) and (c) where an increase in linearity is apparent.

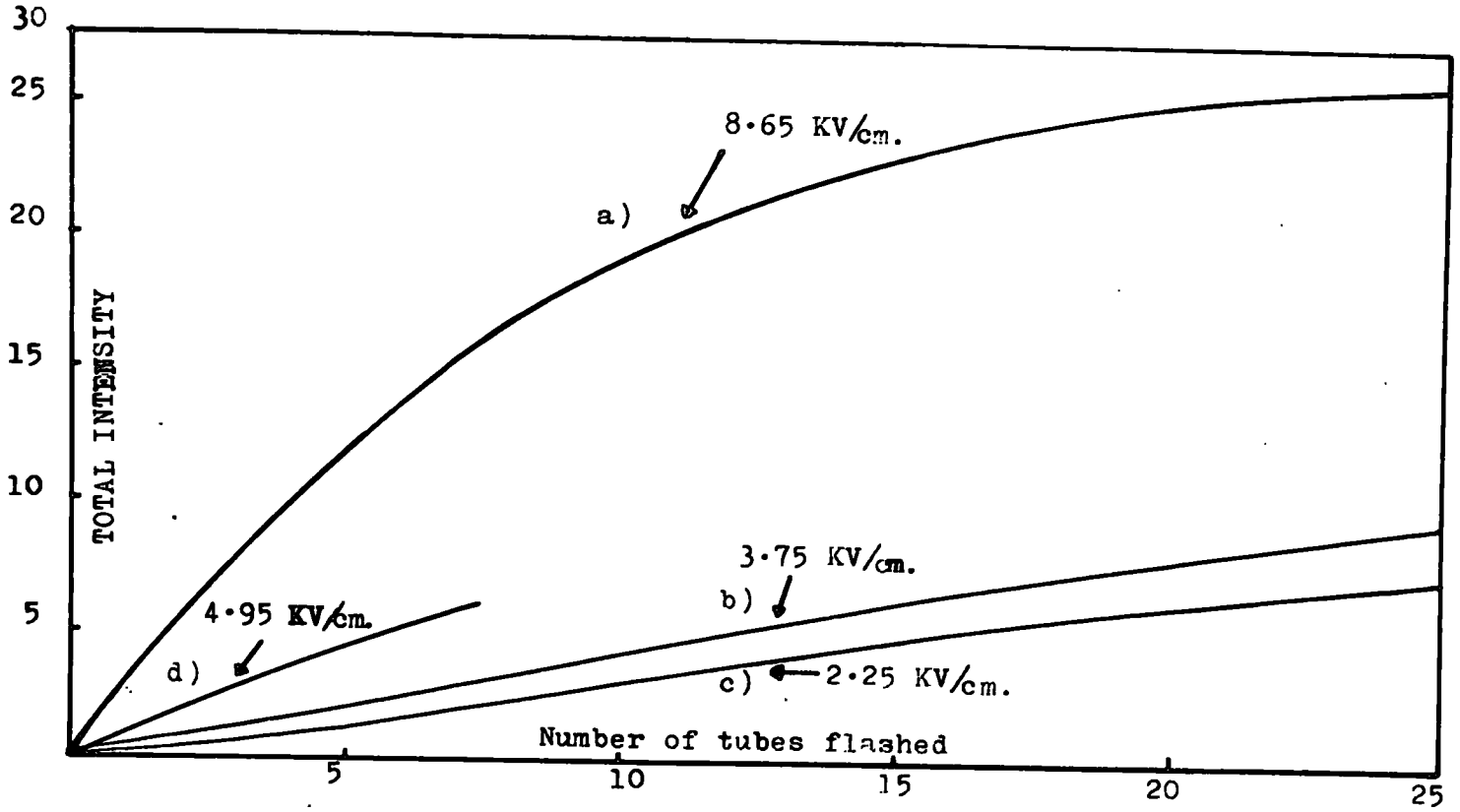

Fig. 3.6. The variation of intensity with number of tubes flashed.

With the array operated under the conditions applied for curves (b) and (c), it should be possible to select events where more than n tubes have flashed by demanding that the pulse height should be greater than a set value. Figure 3.7 shows the discriminator characteristics for $n = 9$ and $n = 14$ assuming that the value of the intensity is $n + \frac{1}{2}$. It is seen that there are events selected which correspond to lower values than the chosen n value and also that some greater than n are missed. This can be ascribed to the fluctuations already discussed. The indications are, however, that the discriminator characteristics are satisfactory.

3.5 Conclusions and Discussion

It has been shown that the measurement of the intensity of the flash of light from a neon flash-tube by a photomultiplier is an accurate measure of the number of tubes flashing in an array of tubes. The disadvantage in the application of this method in the field of extensive air showers is the sharply peaked polar diagram of the long tubes. A considerable path length is required between the array and the photomultiplier. The use of mirrors may be envisaged and the possible use of a translucent material on the front of the tubes. If this can be achieved the photographic recording of the flashes can be dispensed with, and instead, measurements of the pulse heights from a photomultiplier recorded.

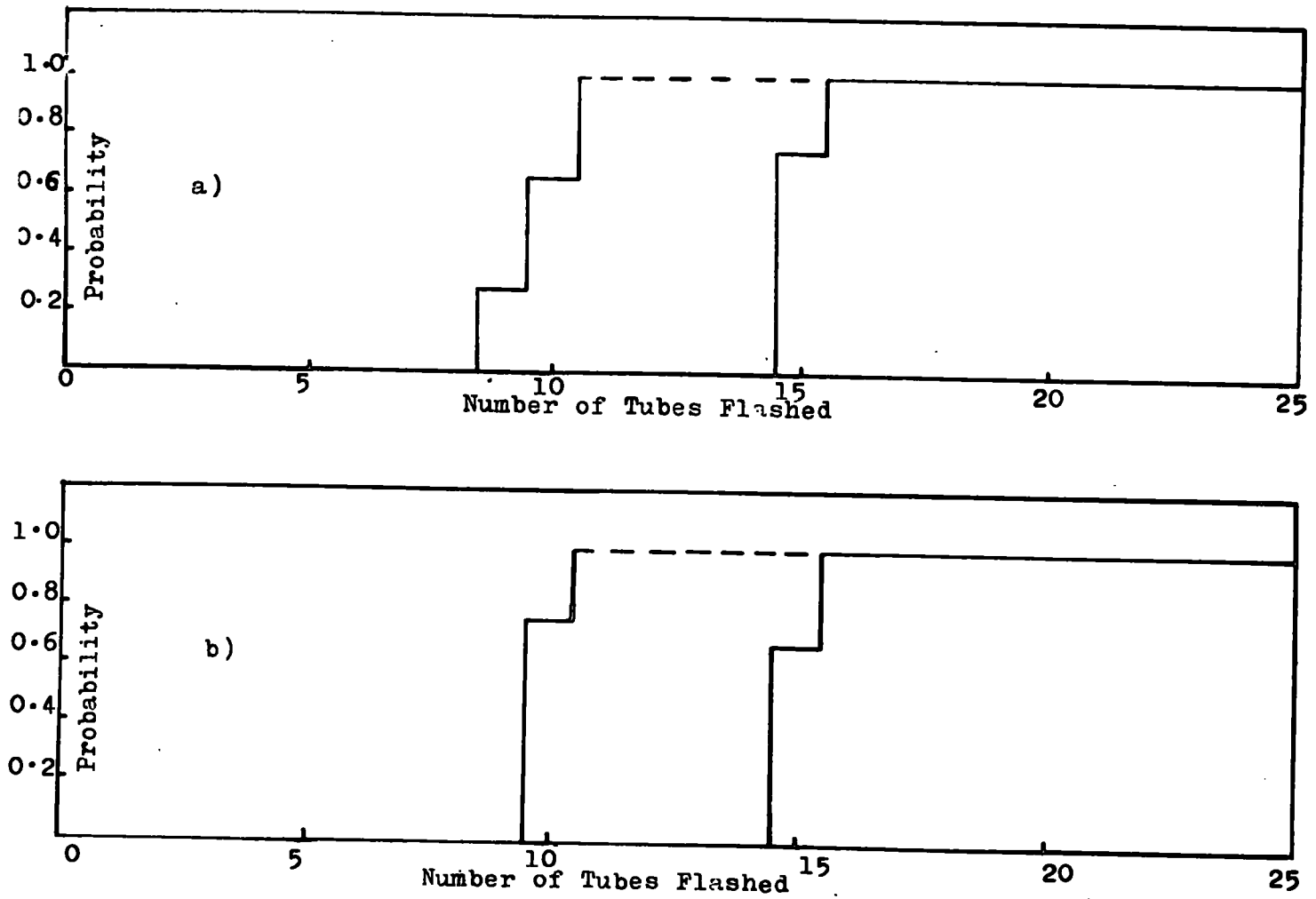

Fig.3.7. The Discriminator Characteristics.

Chapter 4

The Directional Air Shower Indicator

4.1 Introduction

At present studies of extensive air showers are being made mainly by the use of Cerenkov detectors and Scintillation counters. Both these detectors are essentially energy-loss detectors and there is a complicated relationship between the output signal and the number of particles which have passed through them. Effects such as the materialisation of gamma rays, nuclear interactions in the detector and the absorption of low energy electrons must be taken into account. For an accurate determination of particle density it is obviously desirable to use counters capable of counting numbers of particles directly. For this purpose arrays of Geiger counters have been used. Recently, the neon flash-tube technique has been developed and used for this purpose. Fukui et al.(1960) have used an array of flash-tubes below a concrete block equivalent to forty radiation lengths in thickness as a μ-meson detector in their extensive air shower array. A further array of tubes was used by these workers to study the fine structure of the core observed in air showers.

With a neon flash-tube array, having tubes with thin glass walls, there is a close relationship between the number of particles and the number of tubes discharged, provided that the density is not so high that the statistical

correction introduced by the probability of more than one particle passing through a tube is not too great. Hence a more accurate estimate of the density of particles falling on the apparatus is presented.

The use of flash-tubes in the form of a large array has been shown to be suitable for a variety of experiments on showers. The apparatus that is described in this chapter was designed by H. Coxell (1961). Only minor alterations were made for the present experiment which was carried out in collaboration with Imperial College, London at the Silwood Park Field Station, Sunninghill, Berks. The objects were to investigate

1. The Zenith Angle Distribution of Showers of size 10^5 Particles
2. The Density Spectrum of Extensive Air Showers
3. The Calibration of the Cerenkov Detectors
4. The Statistical Distribution of Particles in Showers.

The determination of the density spectrum and the Cerenkov detector calibration were the concern of the author.

4.2 Properties of the Flash-Tubes

The tubes used in the Directional Air Shower Indicator (hereinafter called D.A.S.I.) were of length 115 cms and internal diameter 1.6 cm. In all, the apparatus contained 892 tubes made of Soda glass and filled with Commercial Neon (Table 1) to a pressure of 60 cm Hg. It

has been shown that these tubes exhibit the following properties:-

a) High plateau efficiency,

b) High efficiency at time delays up to 20 μsec.

The characteristics of these tubes are shown summarised in figures 4.1 and 4.2.

Table 1

Composition of Commercial Neon Gas

Neon	98 ± 0.2%
Helium	2 ± 0.2%
Oxygen	10 v.p.m.
Nitrogen	100-200 v.p.m.
Argon	~0.5 v.p.m.

4.3 Geometry of the Array

The array consisted of sixteen layers of tubes, each tube having a sensitive length of one metre and the alternate layers were crossed at right angles to permit measurement of both spatial and projected angles. The extreme trays consisted of four layers of fifty-five tubes whilst the central four trays had two layers each of fifty-six tubes. The uppermost measuring layers consisted in fact of two overlapping single layers and thus presented an effective layer efficiency of 100%. By observing the number of tubes flashed in each layer of this top tray, four estimates

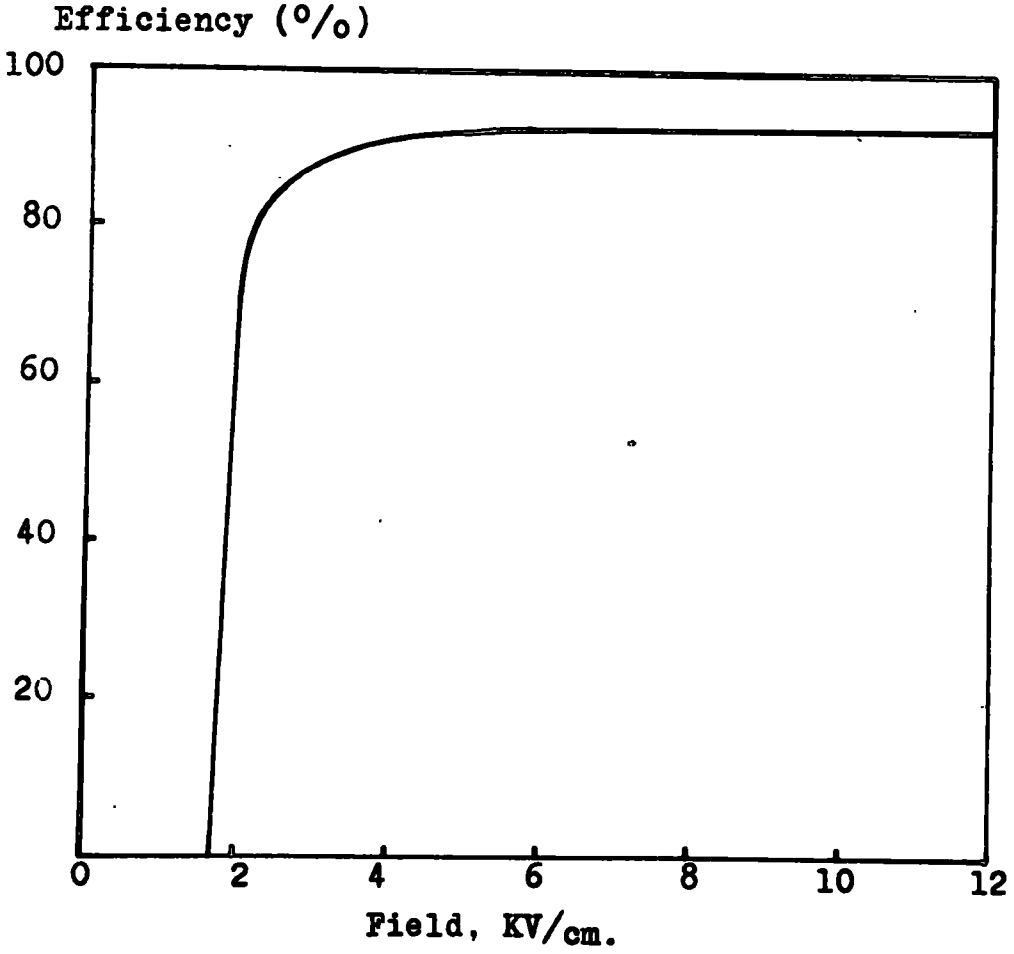

Fig.4.1. Internal efficiency as a function of field strength.

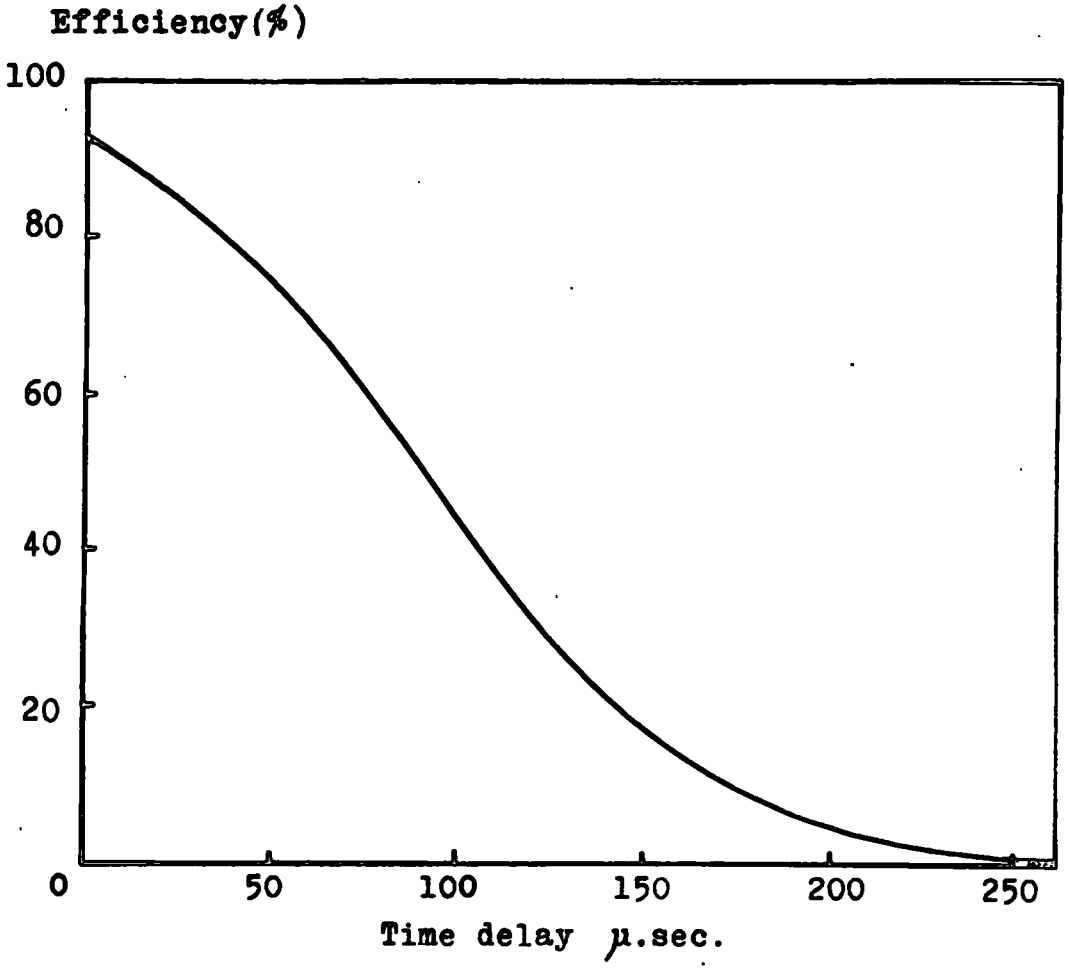

Fig.4.2. Variation of efficiency with time delay.

of the incident particle density could be obtained for each event recorded.

The functions of the four intermediate layers were:-

1. To relate the flashes in the two extreme defining layers.
2. To increase the overall angular resolution.

The separation of the layers was chosen as the result of an analysis by Coxell (1961), who found that as the separation was increased the angular resolution was improved but the maximum density which could be accepted, whilst retaining an unambiguous relationship between the flashes, was reduced. The optimum compromise between the two functions was determined graphically as 13 cm, but for the present experiment a smaller separation was used, sacrificing some degree of angular resolution, to permit observation of higher particle densities. The extreme layers for the Silwood experiment were separated by 70 cm whereas in Durham they had been 100 cm.

4.4 Construction

As consideration was made for the simplest form of construction consistent with efficient performance, each layer was housed in a rectangular frame of 1" Duralumin. No locating grooves were considered necessary, the tubes being stacked side by side and care was taken to obtain parallelism as far as possible. The trays were located in a Handy-Angle framework of size 4 ft. cube. The crossed tubes were located at right angles to an accuracy of $\pm 0.12^{\circ}$.

To keep scattering effects to a minimum within the apparatus electrodes of Aluminium foil were used with Pyrex glass serving as insulators for the positive electrode.

4.5 The Electronic Circuits

For the purpose of this experiment the high voltage pulse was obtained by discharging a condenser into the primary of a pulse transformer. The magnitude of the pulse could be varied by changing the tapping on an impedance chain, which was encapsulated in wax to reduce atmospheric effects. Due to the high electrostatic capacity of each layer of tubes (~900 μF) four trigatron units were used and their outputs through the associated impedance chains were connected in the following manner.

1. A single trigatron unit for each extreme tray.
2. A single trigatron unit for each pair of the middle trays.

The final pulse which was applied to the electrodes had a rise time of 0.3 μsec and a width of 2.5 μsec.

The trigger pulse obtained from the Cerenkov array passed through a Rossi coincidence circuit which controlled the various recording operations and triggered a large hydrogen thyratron (XH8), thus causing the four trigatrons to be discharged. The time delay between the initial triggering of the Cerenkov array and the application of the pulse to the plates of D.A.S.I. was adjusted to 30 μsec.

This long delay was found to be necessary due to the 'pickup' emitted during the discharge of the D.A.S.I. unit which obscured the Cerenkov records.

4.6 Recording

The D.A.S.I. unit was operated in a large trailer and, due to the confined space, mirrors were required so that recording of both faces of the unit could be made using a single Shackman camera (F1.9). A diagram of the layout of the apparatus in the trailer is shown in figure 4.3. Ilford H.P.S. film which is red sensitive was used and the camera was driven electrically by a pulse from the Rossi coincidence unit. For each event fiducial lights were operated to define the vertical axis. A clock was attached to one face of the array and this was illuminated for each event, thus enabling a correlation to be made between the events recorded by D.A.S.I. and those of the Cerenkov array. The total path length between the face of the array and the plane of the film was 350 cms. The mirrors were adjusted such that the distortion of the image was a minimum.

4.7 The Silwood Park Array

The array consisted of four Cerenkov detectors as shown in figure 4.4. D.A.S.I., as is shown in the figure, was situated 23 metres from the centre of the detecting array, so as to be in a region of comparatively low density. The detector spacing for the duration of the

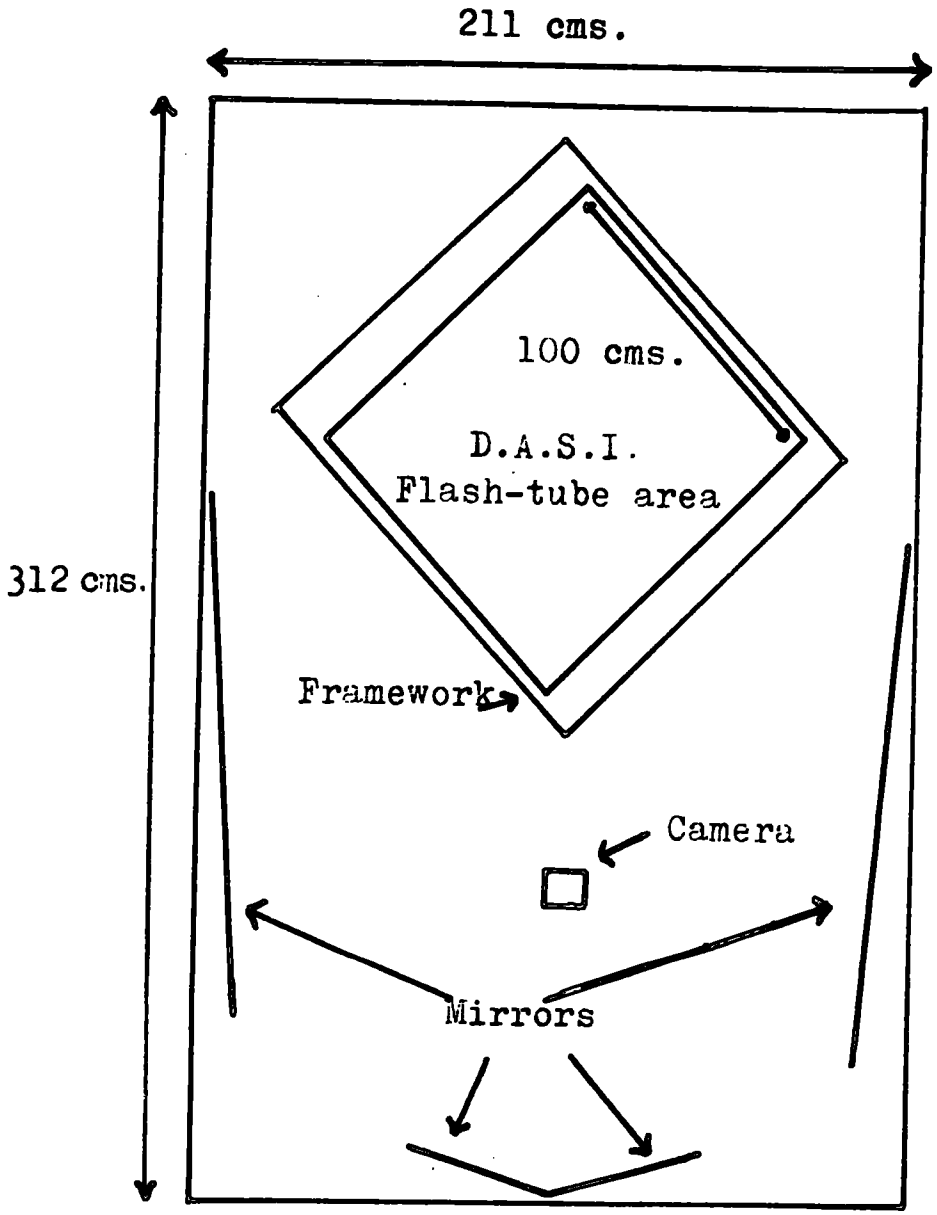

Fig. 4.3. The layout of apparatus in the caravan.

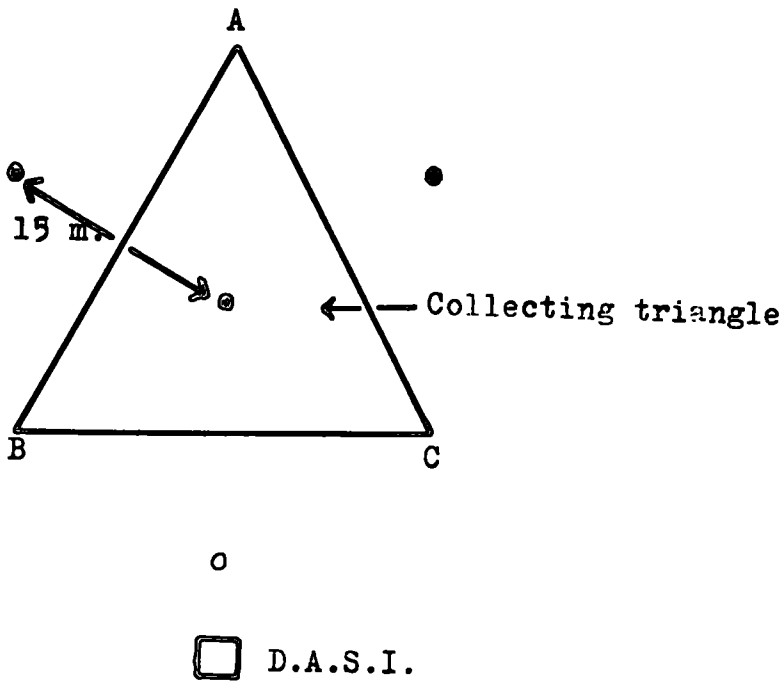

Fig.4.4. The Silwood Park array.

experiment was 15m. Each of the four detectors consisted of a cylindrical tank lined with white P.V.C. ('Darvic'), 1.82 m^2 area, 76 cm deep, and completely filled with water. The Cerenkov light from the shower particles in the water was diffused by the Darvic and about 1% of it reached the photo-cathode of a 5 inch diameter photomultiplier. The pulses from the photomultipliers were successively delayed before being applied to the recording oscilloscope so that the four pulses appeared side by side on the screen. The oscilloscope traces were triggered by a master pulse which was produced when pulses greater than the trigger bias arrived simultaneously from the central detector and two others. This pulse was also used to trigger D.A.S.I.

The showers selected for the determination of the shower-size spectrum represent only a small proportion of the total number of the showers recorded. The collecting area of the Cerenkov array was the triangular area ABC enclosed by the perpendicular bisectors of the lines joining the outer detectors to the central one. In the analysis of the results it was required that the showers should be large enough to trigger the array irrespective of where they fell in the collecting triangle. A further criterion adopted was that showers whose axes were located within 5 m of the central detector were excluded. This was

due to errors in the location of the shower axis which are found to increase the estimated distance. Furthermore, showers whose axes fell close to the edge of the collecting area were excluded unless the central detector showed a significantly larger density than the next (more than one standard deviation). This prevented the inclusion of showers which in fact fell outside the triangle but due to a fluctuation recorded a large density at the central detector.

Only showers that satisfied these criteria were used in the shower-size spectrum and the corresponding events recorded by D.A.S.I. considered in the determination of the density spectrum.

Chapter 5

The Density Spectrum

5.1 Introduction

In a given shower, the particle density varies with the distance from the axis but it is found that the lateral distribution is nearly the same for all showers, so that the particle density at a given distance from the axis is proportional to the total number of particles in the shower. Thus we can write

$$\Delta(r) = N.f(r)$$

where N is the shower size and f(r) is the lateral structure function.

It is known experimentally that the differential frequency spectrum of densities is given by

$$V(\Delta)d\Delta = K\ \Delta^{-\gamma-1}\ d\Delta$$

where $V(\Delta)d\Delta$ is the number of showers per unit time falling on unit area with densities lying between Δ and $\Delta+d\Delta$, and γ is the exponent of the integral density spectrum

$$V(>\Delta) = K'\ \Delta^{-\gamma}$$

The number or size-spectrum of extensive air showers can be written as $\eta(N)dN$; this is the number of showers whose axes cross an area of 1 m^2 at the point of observation in unit time and which contain a total number of particles between N and N+dN. Assuming, as mentioned above, that all showers have the same lateral structure it

can be shown that the differential size spectrum takes the form

$$\eta(N)dN = AN^{-\gamma-1}dN.$$

Thus, the exponent of the size spectrum is the same as that of the density spectrum. There is, furthermore, a relationship between γ and the slope of the primary energy spectrum since N is related to the energy of the primary particle. Therefore, the determination of this exponent, using apparatus such as D.A.S.I. which is capable of giving four estimates of the density for each event, can provide important knowledge in the investigation of properties of extensive air showers. It should be noted that whilst there is comparative simplicity in the determination of γ using D.A.S.I. only the average behaviour of showers is studied, thus the approach is less direct than the determination of the corresponding size spectrum.

5.2 The Method of Measurement of γ using D.A.S.I.

Assuming that the particle density is uniform over the area of the apparatus ~1 m^2, it is possible to determine the most probable particle density Δ, which has discharged a given number of tubes, k, in a layer of tubes, l, each of sensitive area s. This probability is given by

$$P_k = {}^{l}C_k \, (1 - \exp(-s\Delta))^k \, (\exp(-s\Delta))^{l-k} \qquad 5.1$$

From this is obtained the relation

$$\Delta_k = \frac{1}{s} \ln \frac{l}{l-k} \qquad 5.2$$

where Δ_k is the most probable density resulting in k tubes having been flashed. The application of this relation is limited and a reasonably accurate determination of Δ can be made only within the requirements that $1-k>2$ and $k>3$. The curve in figure 5.1 shows the variation of $s\Delta$ with k for values of $k = 3$ to $k = 53$. The particle density corresponding to the number of tubes flashed in each layer can be obtained directly from this curve. In the determination of the density spectrum account must, however, be taken of the change in cell width of density with k,

$$\nu(s\Delta) = N(k) \frac{dk}{d(s\Delta)} \qquad 5.3$$

Accordingly, $\frac{dk}{d(s\Delta)}$ is plotted as a function of $s\Delta$ in figure 5.2. This method, though limited at both high and low densities, does give a reasonably rapid indication of the value of γ.

5.3 The Sensitive Area of the Flash-Tube

The sensitive area of the flash-tube is dependent upon the length, L, of the electrode, the internal diameter of the tube, d, and the internal efficiency of the tube η_{int}. Two efficiencies of the flash-tube can be defined:

1. the layer efficiency, η_1, which is the ratio of the number of single flashes observed in a layer to the number of single particles that have passed through that layer,
2. the internal efficiency, η_{int}, derived from η_1 by multiplying by the ratio R of the separation of the

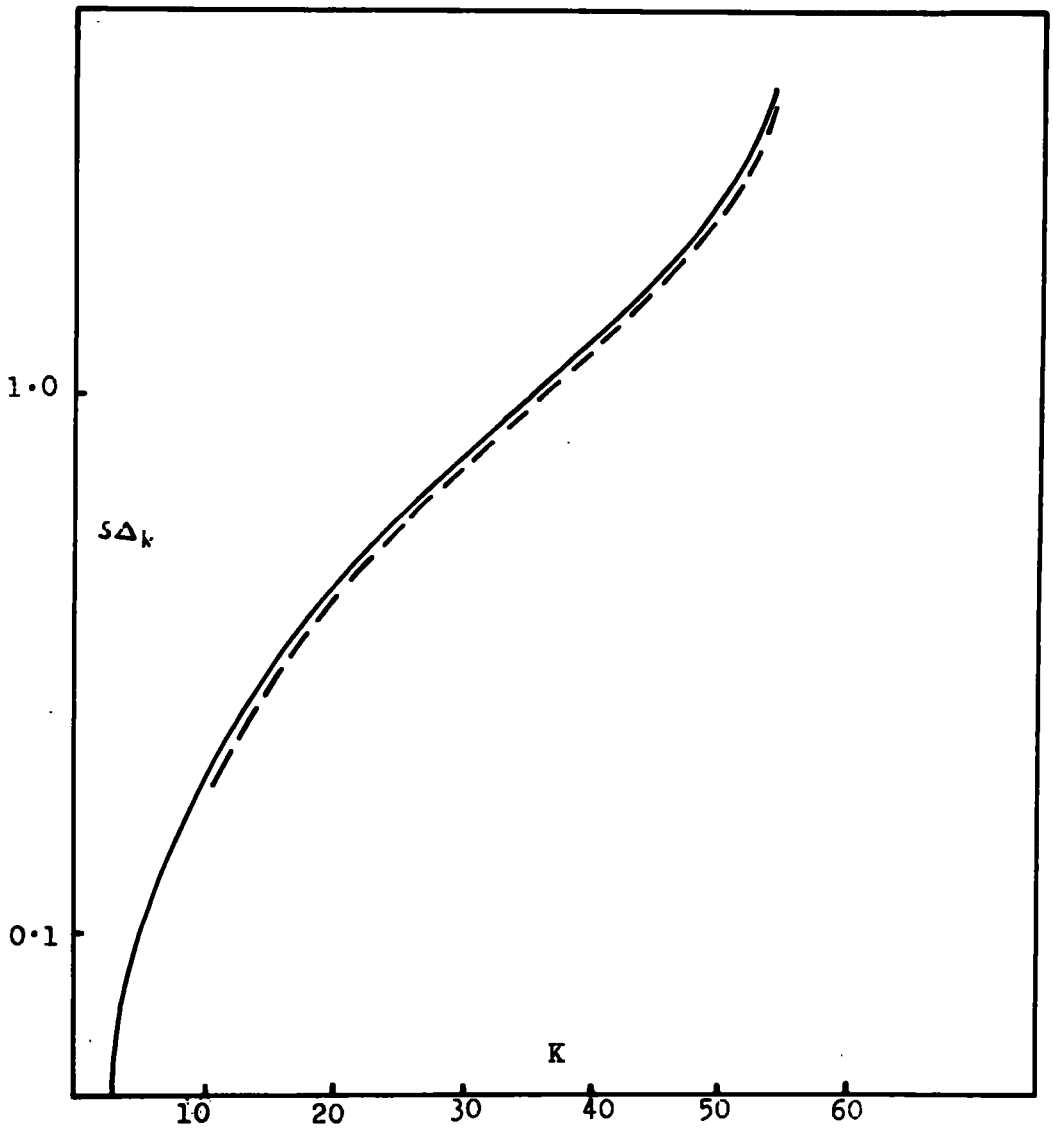

Fig. 5.1. Curve showing the most probable density Δ_k resulting in K tubes having been flashed (S being the sensitive area of the tube)

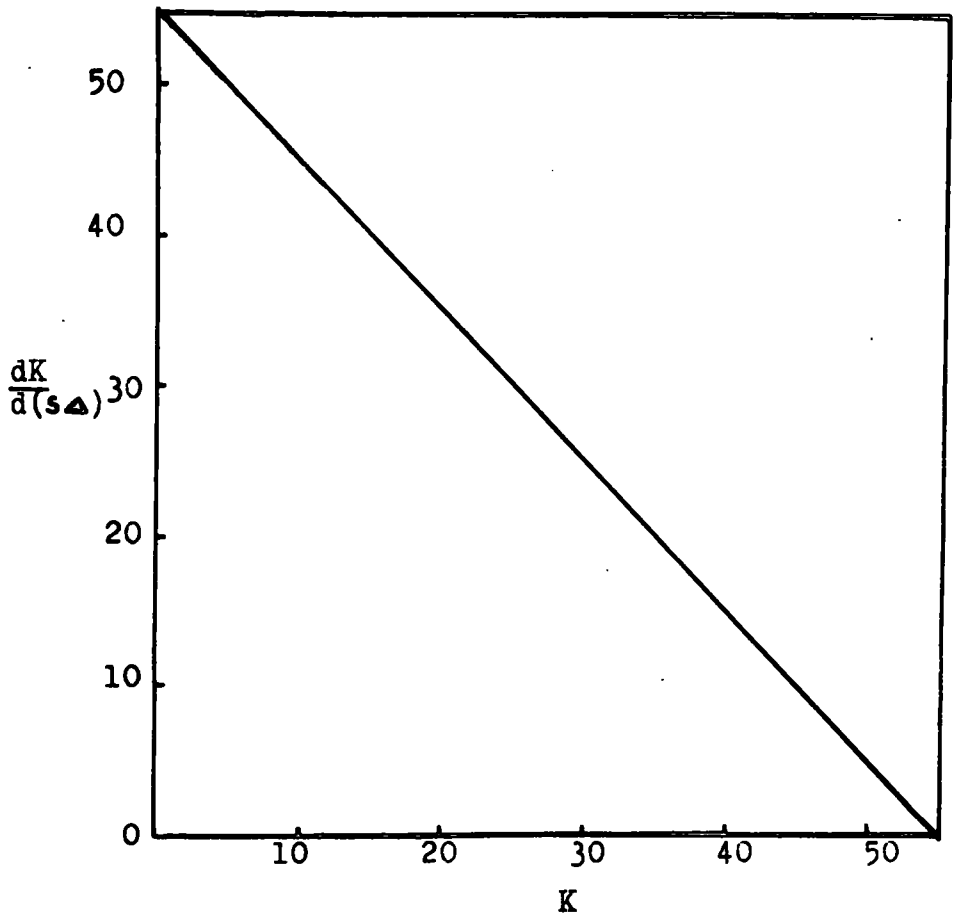

Fig.5.2. Variation of cell width of $S\Delta$ with K.

tube centres to the internal diameter of the tubes. This definition involves the reasonable assumption that only those particles traversing the gas in a tube can cause a flash in that tube. For the determination of the layer efficiency of D.A.S.I. a simple three-fold Geiger counter telescope was used to select particles fully traversing the array. At a time delay of 30 μsecs the apparatus was found to be operating with a value of $\eta_1 = 70\%$. The corresponding internal efficiency of the tube is 79% which compares with the value of 83% obtained using a test array of twenty-five tubes (figure 4.2). This slight discrepancy is not unexpected. The sensitive length is 101 cm. The sensitive area is given by the equation

$$s = L.d.\ \eta_{int}\ cm^2 \qquad 5.4$$
$$= 1.28 \times 10^{-2}\ m^2.$$

5.4 The Accurate Determination of γ

The above method of determining the density spectrum does not take into account the effect of the slope of the incident spectrum upon the relationship holding between particle density and the number of tubes that have flashed. A more accurate treatment is therefore required; such a treatment is also needed for the extreme density measurements which are not included in the method already outlined.

The spectrum shown in figure 5.3 was used as a trial spectrum and the expected frequencies of k tubes having

flashed was computed and compared with those observed. The trial spectrum was then successively modified until agreement was reached between the expected and observed frequencies. The adopted spectrum was then that which gave the best fit.

The accurate treatment is as follows; considering an incident spectrum of the form $\nu(\Delta)d\Delta$, the chance of observing any combination of k tubes being flashed by an incident particle density of Δ to $\Delta+d\Delta$ is given by,

$$R_k d\Delta = {}^{l}C_k \left(1 - \exp(-s\Delta)\right)^k \left(\exp(-s\Delta)\right)^{l-k} \nu(\Delta)d\Delta$$

i.e.

$$R_k d\Delta = G\,{}^{l}C_k \left(1 - \exp(-s\Delta)\right)^k \left(\exp(-s\Delta)\right)^{l-k} \Delta^{-\gamma-1}\, d\Delta \qquad 5.5$$

if we write $\nu(\Delta)d\Delta = G\,\Delta^{-\gamma-1}\,d\Delta$.

(It must be noted that this form is applicable only at such high densities where bias effects, introduced by the size of the detecting array, are negligible). Probability curves derived from equation 5.5 are shown in Fig. 5.3. The R_k curves in figure 5.4 are obtained by multiplying the P_k curves by the assumed spectrum. Two effects may be noted:-

1. The R_k curves peak at new values of $s\Delta$ which are shown in figure 5.1 by the dotted curve.
2. The areas under the curves are altered.

The areas of these curves give directly the relative frequencies of the various numbers of tubes being discharged.

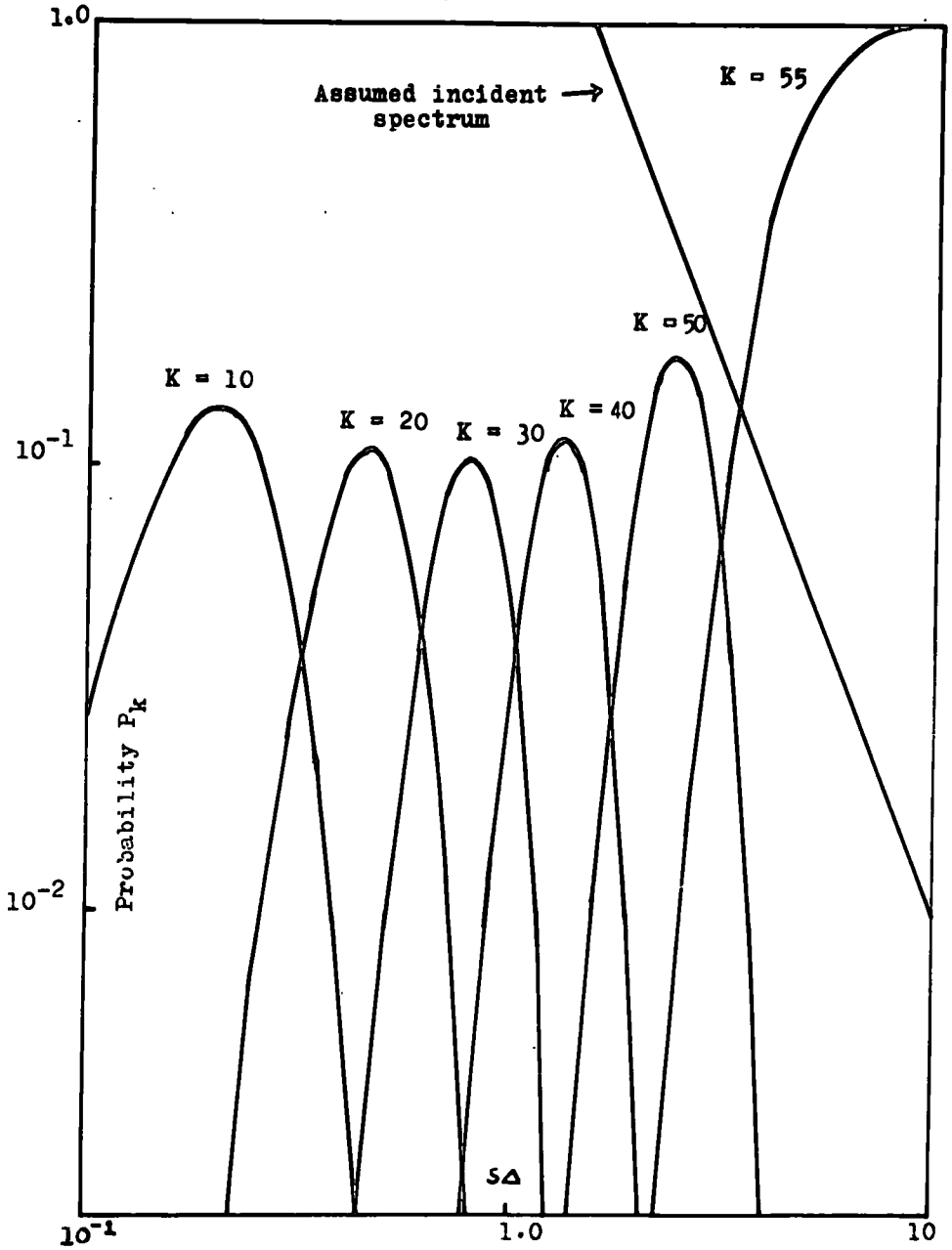

Fig.5.3. The probability that a shower of density Δ discharges K counters in a layer of 55 counters.

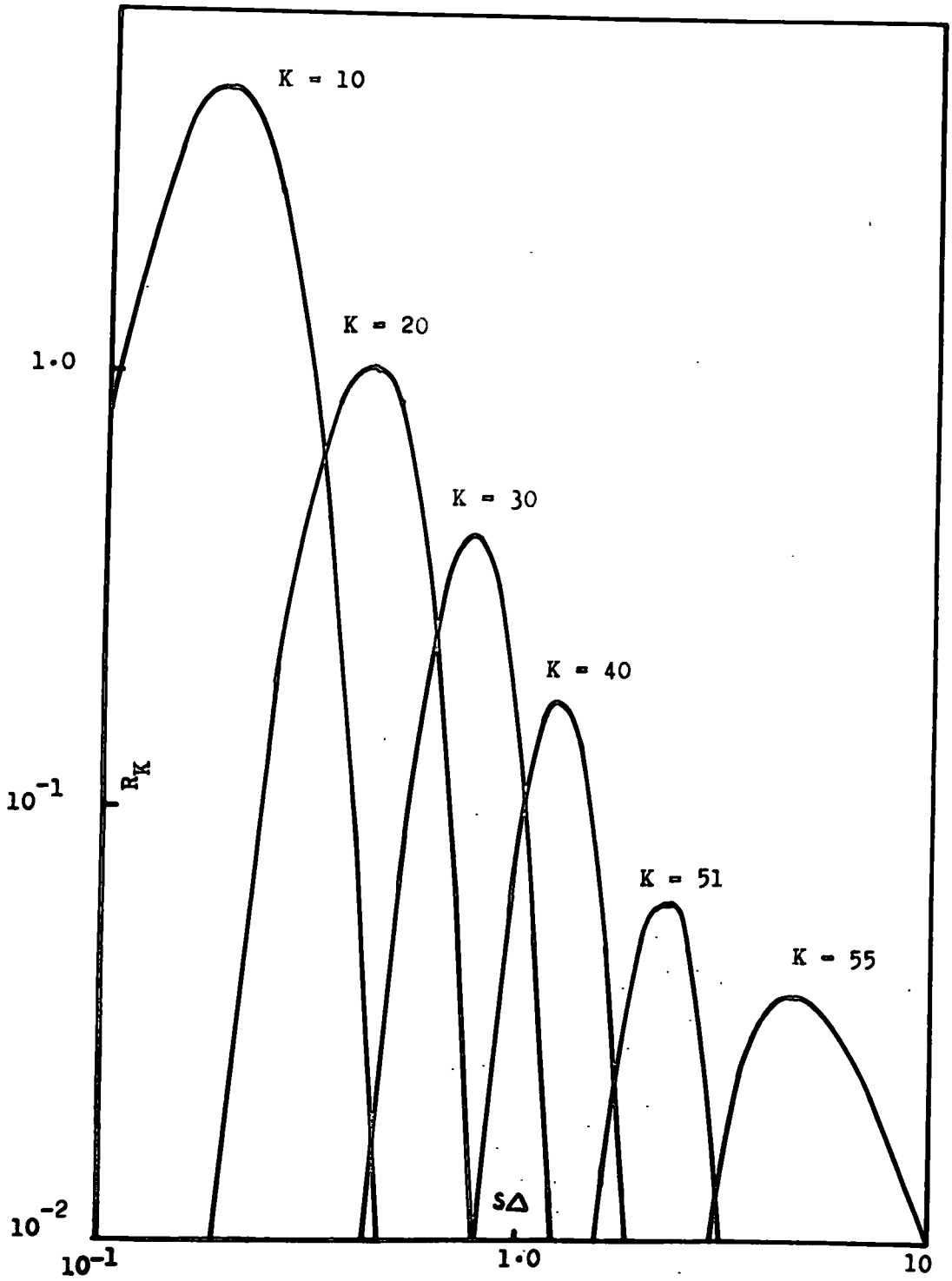

Fig.5.4. **The effect of applying the assumed incident spectrum to P_K curves.**

The absolute contributions are obtained by summing the areas under the R_k curves and normalising to the observed total number of events recorded. The best-fit incident spectrum is determined by multiplying the frequency of the assumed spectrum at each value of density by the ratio of the observed to expected frequency at that density. The errors are evaluated using Poisson and Fiducial Limits in observed frequencies, Regener (1951).

5.5 The Measured Values of γ

5.5.1 The Durham Experiment

Preliminary tests of the D.A.S.I. unit were carried out in Durham by Coxell (1962). The shower selection system comprised three trays of Geiger counters, each of area 0.126 m^2, arranged round the array on a circle of 1.9 m radius. The differential density spectrum obtained is shown in figure 5.5. A value of $\gamma + 1 = 2.61 \pm 0.05$ was obtained by means of a least squares fit to the experimental points at densities greater than 40 particles/metre^2. The measured spectrum departs from the incident spectrum at values lower than this due to the fact that at low densities a bias is introduced by the necessity that there should be at least one particle through each of the counter trays. The integral spectrum is given by

$$\nu(>\Delta) \propto \Delta^{-1.61 \pm 0.05}$$

corresponding to showers of mean size $\bar{N} = 10^5$ particles.

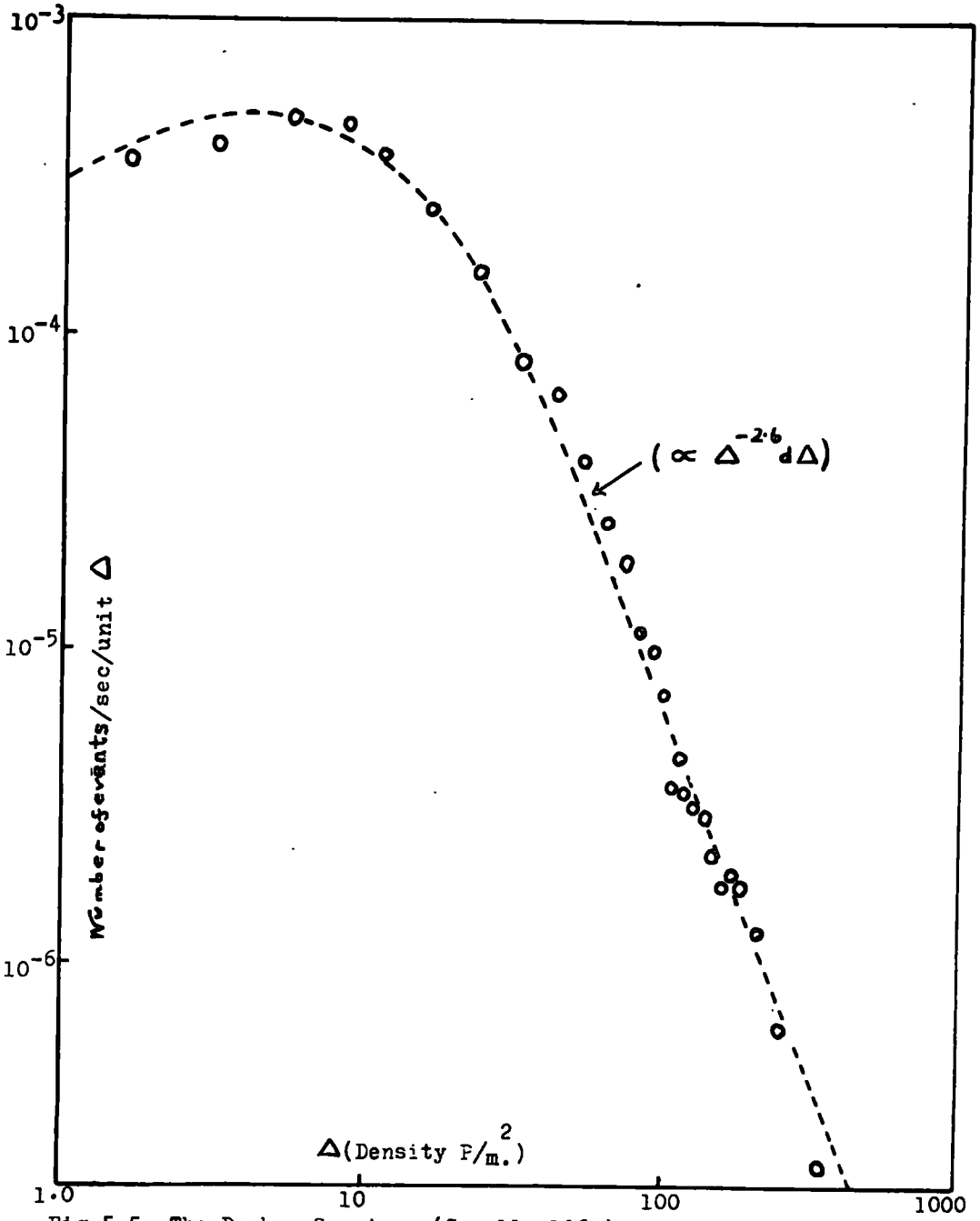

Fig.5.5. The Durham Spectrum (Coxell, 1961).

5.5.2 The Silwood Experiment

Although 2000 showers were recorded, in only 194 cases was it possible to give an accurate location for the core of the shower through its falling within the collecting triangle of the Cerenkov detectors. The differential spectrum obtained is shown in figure 5.6 where the slope $(\gamma+1)$ is 3.3 ± 0.3 over the range of densities studied. The integral density spectrum may thus be represented as

$$\nu(>\Delta) \propto \Delta^{-2.3 \pm 0.3}$$

The information from the Cerenkov array indicates that this value of γ corresponds to a mean value of 9×10^5 particles.

5.5.3 Sources of Error

These have been fully discussed by Coxell (1961). Careful inspection of the flash-tubes was made to ensure that none were damaged during the assembly of the array at Silwood and tubes which flashed repeatedly on the application of random pulses were removed. Care was also taken during the development of the films to ensure that all the flashes were clearly visible over the full extent of the measuring layer. The mis-counting of tubes, especially at high densities, could cause a change in the slope of the spectrum. For the analysis of the events the top layers were divided into four sections and by totall-

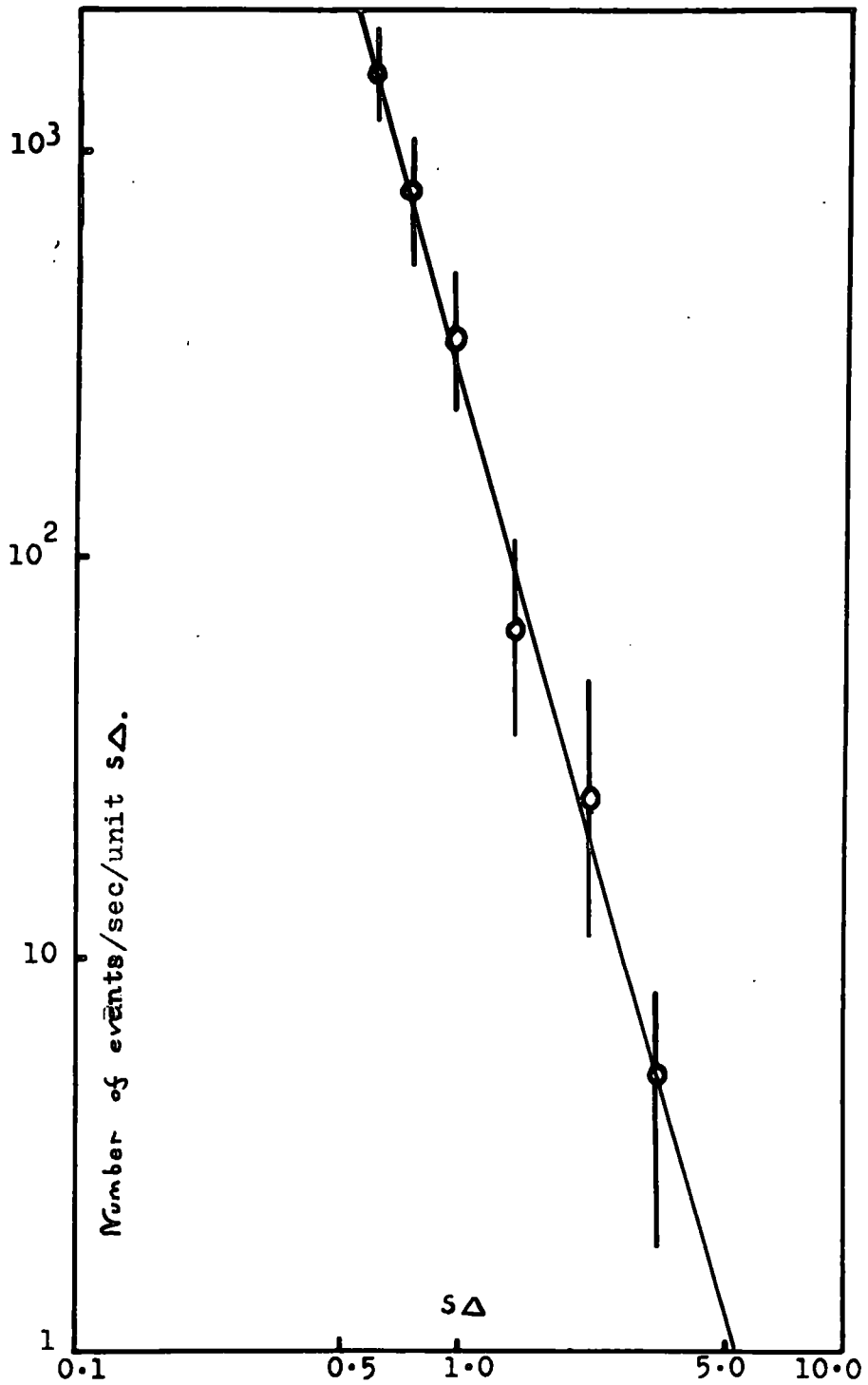

Fig.5.6. The Silwood Spectrum.

ing each section a ready check was obtained on the accuracy of the counting of the number of flashes. As a result observational errors are unlikely.

It has been assumed for the experiment that the density of particles over the apparatus is constant. For this assumption to be valid, the cores of the showers contributing to the determination of the slope of the spectrum must be far removed from the detector. In fact, the showers considered had cores in the range 15 - 37 m from D.A.S.I. and the bias due to variation of particle density across the apparatus was considered to be negligible. It is concluded that the effects of known sources of systematic error are insignificant.

5.6 Discussion and Conclusion

The values of γ found at Durham and Silwood suggest strongly that there is an increase in the slope of the size spectrum of showers between 10^5 and 10^6 particles. Such an increase has been found by other workers (Table 2) and the present work can be regarded as giving support for this important result using a different technique.

Table 2 shows the different values of the slope of the differential size spectrum together with the value of shower size at which this change takes place as obtained by various workers. (N_c').

Table 2

	Allan et al. (1962)	Fukui et al. (1960)	Kameda et al. 2770 m (1960)	Khristiansen (1958 and 1960)	Coxell (1962)
γ_1	2.3 ± 0.1	2.4 ± 0.1	2.55 ± 0.1	2.5 ± 0.1	2.6 ± 0.05
γ_2	3.0 ± 0.15	3.0 ± 0.2	3.04 ± 0.1	3.2 ± 0.3	3.3 ± 0.3
N_c	6×10^5	10^6	4×10^5	8×10^5	10^5-10^6

A 'kink' in the differential density spectrum has recently been reported by McCusker (1961) with values of $-(\gamma+1) = -2.6 \pm 0.3$ for densities in the range 200 - 1000 particles/metre^2 and $-(\gamma+1) = 4.0 \pm 0.5$ for densities greater than 1000 particles/metre^2 which is consistent with the results obtained by Norman (1956) and Prescott (1956). Although the present results at Silwood give the higher slope at densities far below 500 particles/metre^2, there is no inconsistency between the results because whereas the experiments of McCusker were carried out using an unbiassed array, the present work demanded that the shower cores should fall in a prescribed region. in effect it was the number spectrum rather than the density spectrum that was determined at Silwood.

The implications of this change of slope which seems to be well confirmed is that there is possibly a change in the slope of the primary spectrum or that there

may be a change in the characteristics of the high energy nuclear interactions.

Chapter 6

The Calibration of Cerenkov Detectors using D.A.S.I.

6.1 Introduction.

The purpose of the Imperial College experiment was to make a detailed study of the size spectrum of extensive air showers in the region of shower sizes 3×10^5 to 5×10^6 particles. For calibration purposes two trays of Geiger counters were placed on each detector and coincidences recorded together with the heights of the associated Cerenkov pulses. Comparison was then made between the observed and expected pulse height distributions using the appropriate probability function:

$$P(\Delta) = (1 - \exp(-s\Delta))^2 \qquad 6.1$$

This method is, however, statistical in nature in that the results are averaged over several hundreds of events and accuracy is difficult to achieve. The use of a detector such as D.A.S.I., which provides a fairly accurate and direct measurement of the particle densities for each shower that is observed, should provide a good method of checking the calibration of the Cerenkov detectors in individual events.

6.2 Experimental Method

The position of the shower axis was located from the four measurements of the Cerenkov detectors using the lateral structure function appropriate to the detector response (this function does not involve a knowledge of

the calibration). An estimate of the particle density for each shower was provided by D.A.S.I., and knowing the distance of D.A.S.I. from the shower axis, it was possible to calculate the expected shower size N_D. This was compared with the shower size obtained from the Cerenkov counters N_C. The structure function adopted for the calculations was that due to Abrosimov (1960). A check was carried out on this function (see 6.4).

6.3 Discussion of Results

For each of the 191 events considered, estimates of the shower size were obtained from D.A.S.I., N_D, and from the Cerenkov detectors, N_C. Figure 6.1 shows the distribution of relative frequency of showers as a function of the ratio of sizes N_D and N_C. The various parameters characterizing the distribution are given in Table 3.

The data were also considered in three density ranges to determine whether there was any significant change in the response of the Cerenkov detectors to particle number with shower size. The distributions are shown in figure 6.2 and the median values of the ratios N_C/N_D are given in Table 3. A further check was carried out by studying the variation with distance from the core (Figure 6.3 and Table 3).

It is known that there are fairly large fluctuations in density measurements in showers which give rise to

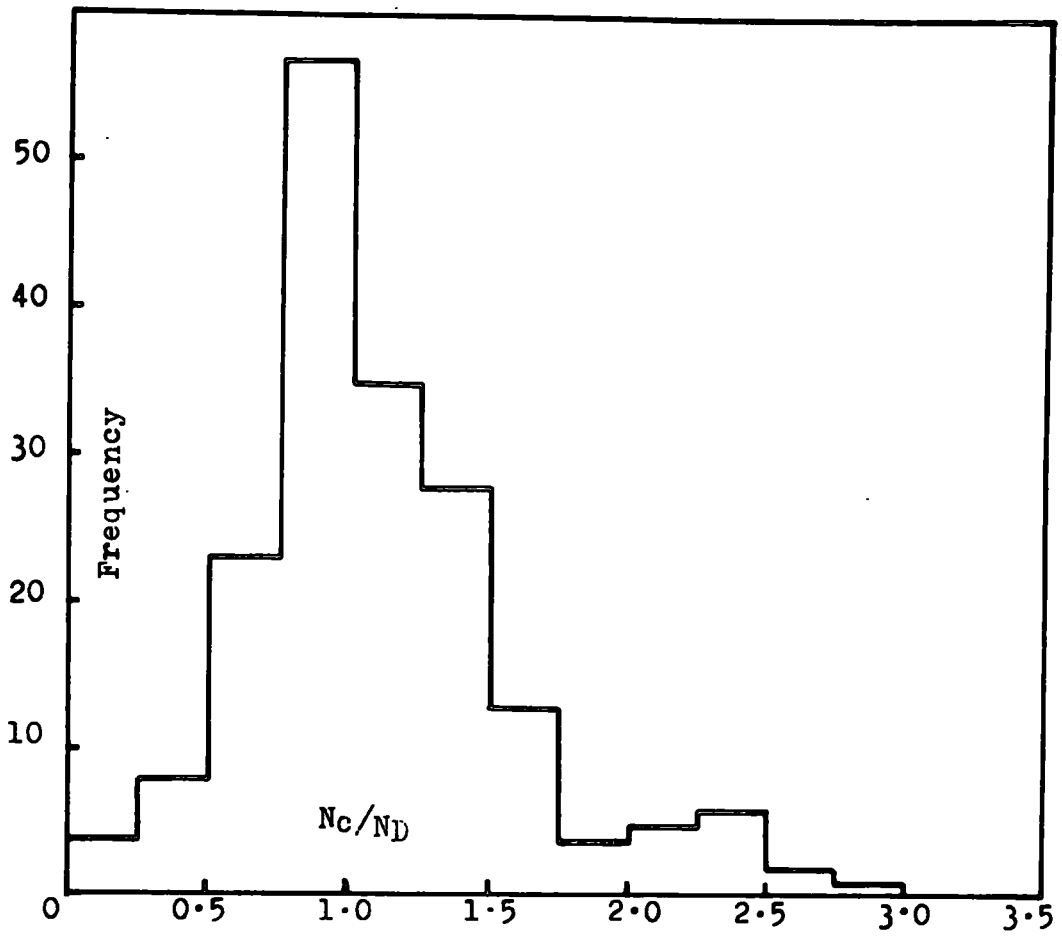

Fig.6.1. The distribution of relative frequency of showers as a function of the ratio of sizes N_c/N_D

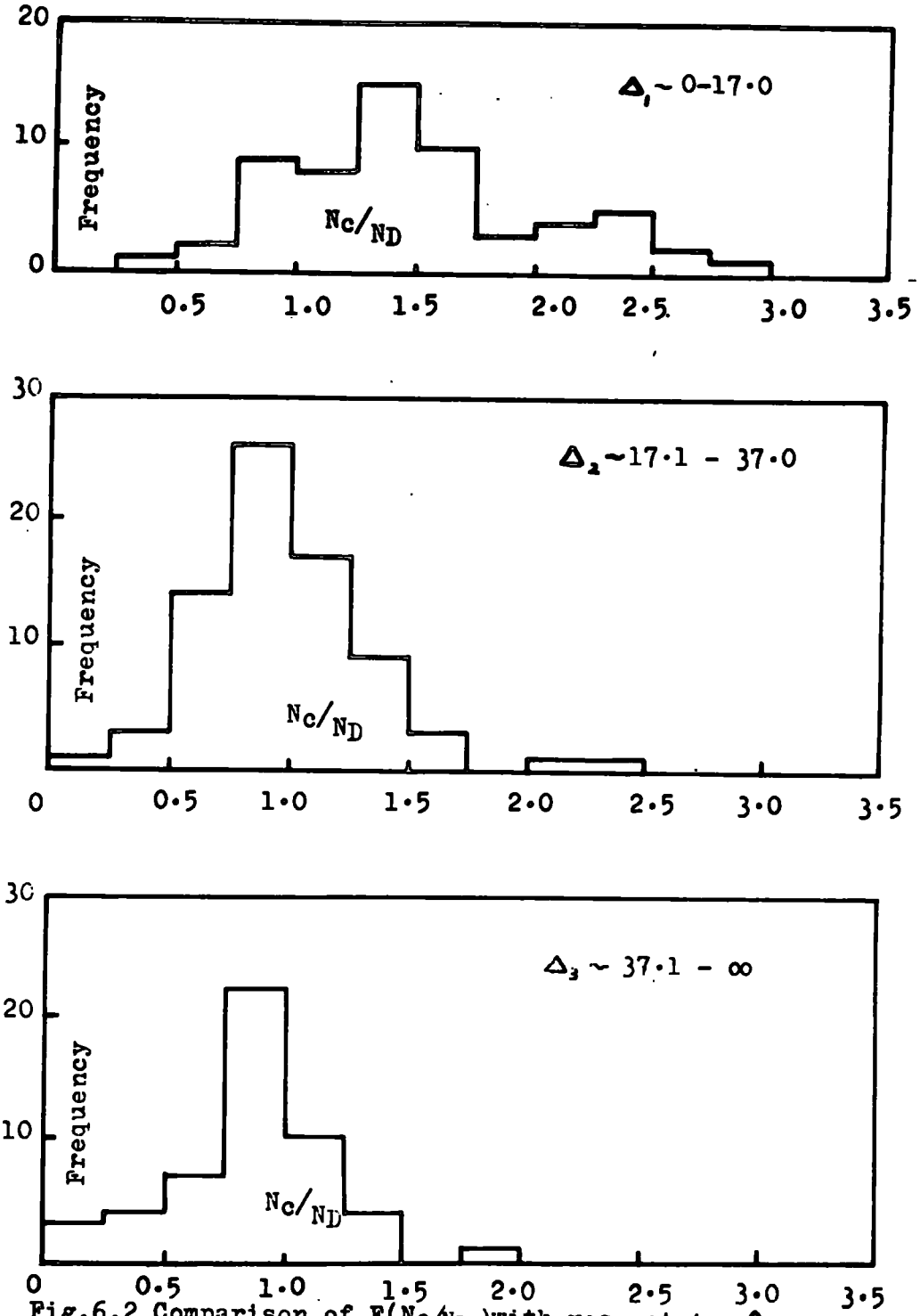

Fig.6.2 Comparison of $F(N_c/N_D)$ with respect to Δ.

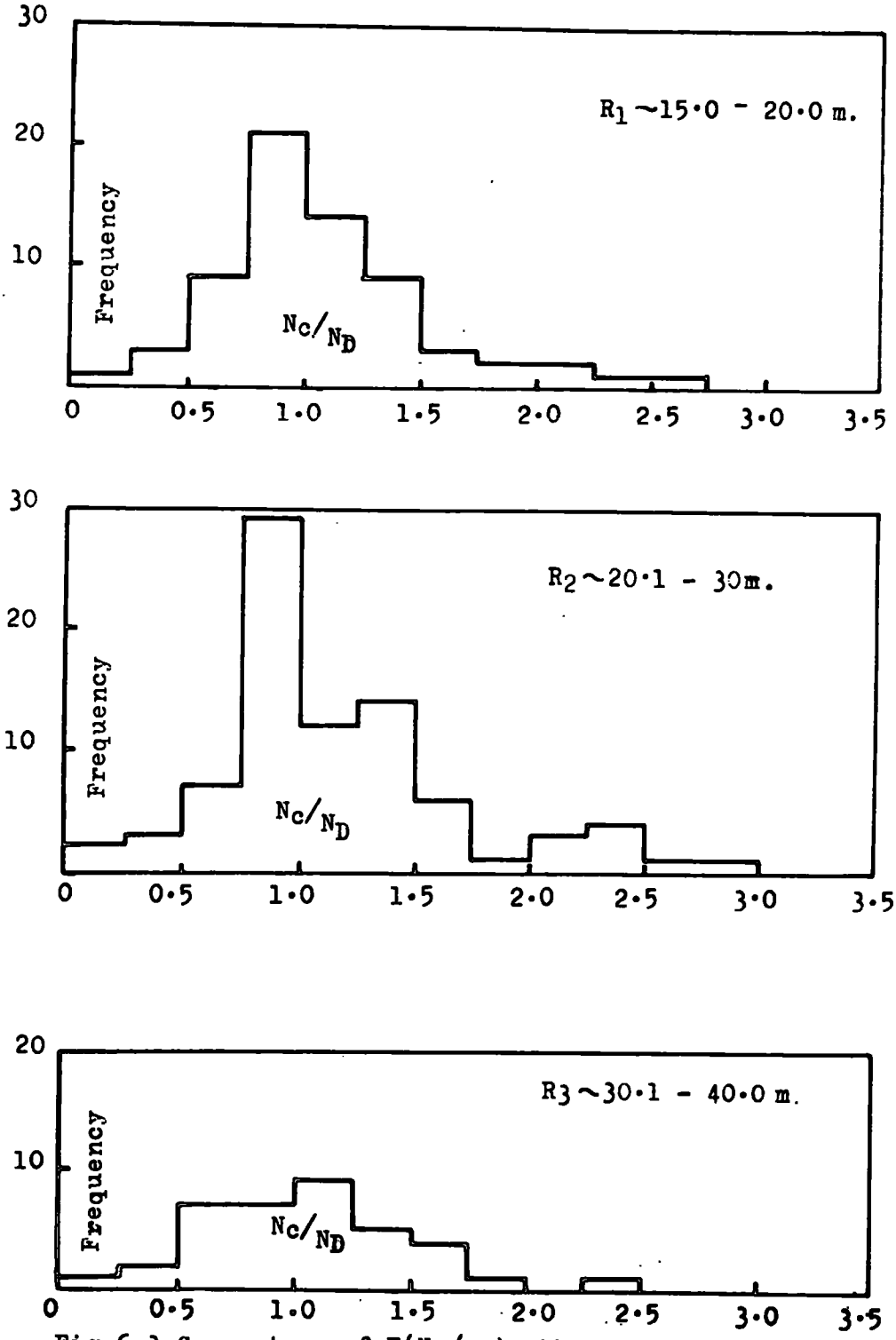

Fig.6.3 Comparison of $F(N_c/N_D)$ with respect to R.

Table 3

Comparison of $F(N_C/N_D)$ with N_C/N_D

	Number of events	Mean	Median	Approx. error	
Total events	191	1.12	1.01	$\pm$0.05	fig. 6.1
Δ_1 = 0-17.0	64	1.49	1.45	$\pm$0.12	fig. 6.2
Δ_2 = 17.1-37.0	76	0.98	0.94	$\pm$0.08	fig. 6.2
Δ_3 = 37.1 - ∞	51	0.85	0.88	$\pm$0.06	fig. 6.2
R_1 = 15-20.0	68	1.07	1.00	$\pm$ 0.08	fig. 6.3
R_2 = 20.1-30.0	85	1.17	1.02	$\pm$0.06	fig. 6.3
R_3 = 30.1-40.0	38	1.06	1.06	$\pm$0.16	fig. 6.3

incorrect size measurements. In plotting the size spectrum from the Cerenkov detector measurements it is endeavoured that in a given size interval the fluctuations are such that the number of smaller showers which fluctuate upwards into that interval about equal the number of larger showers which fluctuate downwards. It will be shown later that this compensation is not perfect.

There appears to be a discrepancy between histogram Δ_1 and histograms Δ_2 and Δ_3 which shows that there is a probable bias introduced in the selection of showers which show a low density at D.A.S.I. This instrument only examines showers if the Cerenkov array shows them to be greater than a certain size. Due to the selection criteria used in the analysis of the results the explanation

of this discrepancy is that in this region of low density showers of size N_C are accepted for the size spectrum determination if larger than N_D but not if they are smaller. Thus showers with $N_C/N_D < 1$ are biassed out.

The histograms for $F(N_C/N_D)$ vs (N_C/N_D) for different ranges of R show that the structure function f(r) due to Abrosimov is satisfactory.

The discrepancy found between the Cerenkov data and the measurements made by D.A.S.I. shows that there is a significant uncertainty in determinations of density using a Cerenkov array. The effect of this uncertainty on the determination of the size spectrum will now be examined.

The frequency distribution shown in figure 6.1 results from the error in determination of size by the Cerenkov detector and that by the flash-tube unit. It is estimated that the results from D.A.S.I. are twice as accurate as those from the Cerenkov array, so to a first approximation the distribution of N_C about N is found by narrowing the N_C/N_D distribution by a factor $\sqrt{\frac{4}{5}}$. The area must first be normalised to unity and the probability $P(R)_i$ of observing a shower of size N_C due to an incident shower of size N is obtained (where $R = N_C/N$). If the true size spectrum is represented by $f(N)dN$, the observed spectrum in N_C is given by

$$f(N_C)dN_C = \int_N f(N)dN.P(R)dR. \qquad 6.2$$

On substituting in (6.2)

$$f(N)dN = KN^{-\Gamma}dN \qquad \text{where } \Gamma = \gamma+1$$

$$f(N_C)dN_C = \int_N KN^{-\Gamma}dN\ P(R)dR$$

$$= \int_N K\left(\frac{N_C}{R}\right)^{-\Gamma} dN\ P(R)dR$$

$$= K\ N_C{}^{-\Gamma}dN_C \int_R R^{\Gamma-1}\ P(R)dR$$

$$= K\ N_C{}^{-\Gamma}dN_C\ F(\gamma)$$

The ratio of observed to real frequencies is then given by

$$\frac{f(N_C)dN_C}{f(N)dN} = F(\gamma) \qquad 6.3$$

or,

$$f(N)dN = f(N_C)dN_C.G(\gamma) \quad \text{where } G(\gamma) = \frac{1}{F(\gamma)}$$

The function $G(\gamma)$ will vary with N_C if there is a change in the slope of the size spectrum. Figure 64 shows the variation of $G(\gamma)$ with N_C if the slope of the spectrum changes from 1.3 to 2.0 at the three assumed values of N. This function may then be applied to correct the observed Cerenkov data so that a more accurate representation of the size spectrum may be obtained. The conclusion that can be drawn from this work is that the Cerenkov detectors give quite an accurate estimate of the true shower size. The magnitude of the correction is comparatively small when viewed against the statistical errors encountered in

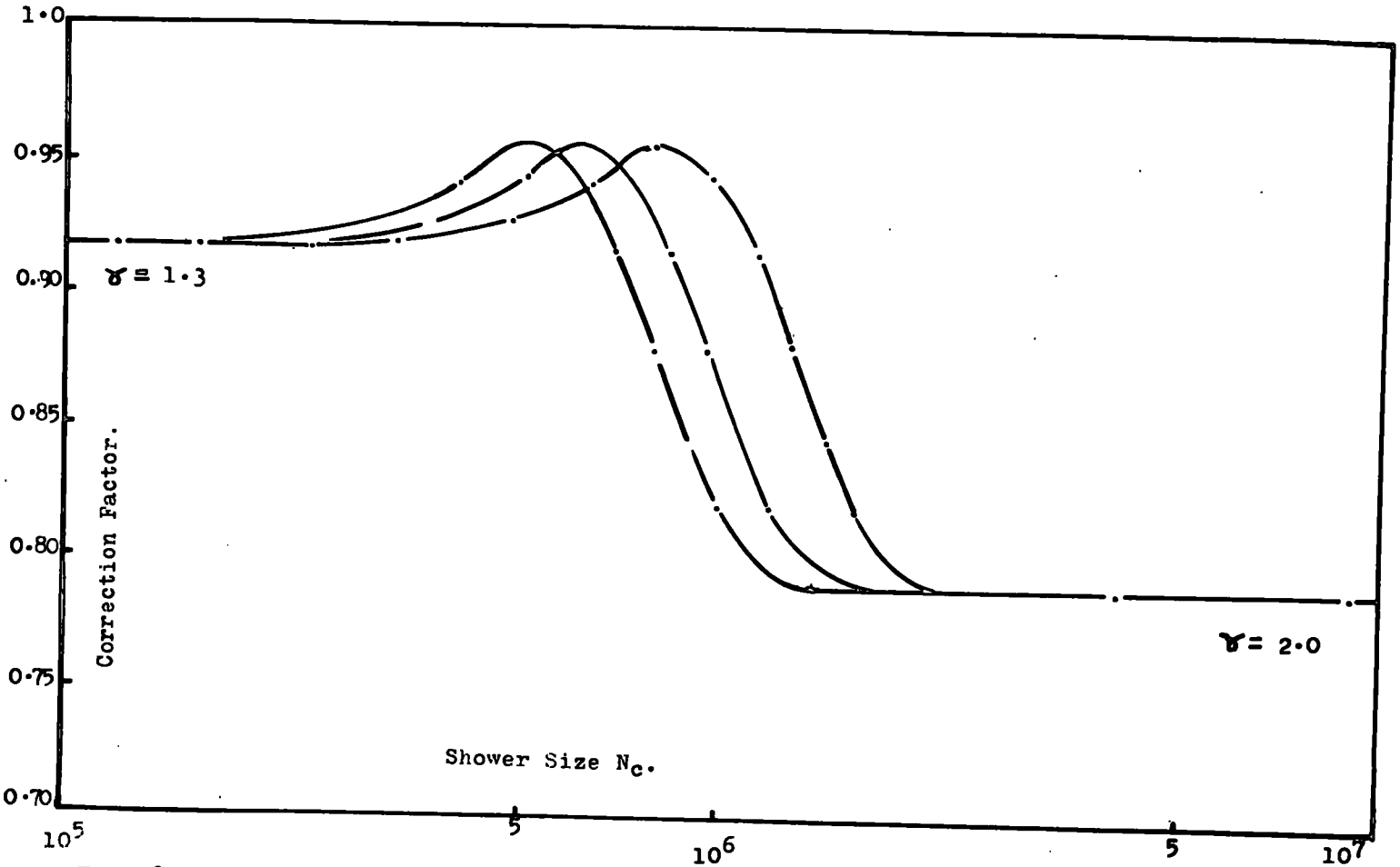

Fig: 6.4. Effect of distribution of $N_c/_N$, Kink as parameter at Nc - 5 x 10^5, 6 x 10^5, and 8 x 10^5.

measurements to date (Allan et al.1961, 62) but significant corrections will be necessary when more extensive data are accumulated.

6.4 The Experimental Verification of the Assumed Shower Function

From the density measurements using D.A.S.I. and the information as to shower core position and size supplied by the Cerenkov detectors, it is possible to perform a direct check on the assumed structure function f(r). This is defined as

$$f(r) = \frac{\Delta(r)}{N}$$

where $\Delta(r)$ is the particle density at a distance r from the shower core observed by D.A.S.I. and N is the shower size determined by the Cerenkov detectors. Figure 65shows a comparison between the results obtained in this experiment together with the structure function of Abrosimov et al.,(1960) where,

$$f(r) = 2.10^{-3}. \frac{e^{-r/60}}{r} .$$

The agreement is reassuring although the range is somewhat limited. Only events located inside the acceptance area of the array were considered. For the determination of the shower size the structure function of Abrosimov et al, was effectively normalised at 24 m due to the use of this function for the 'absolute' calibration of the Cerenkov size determination.

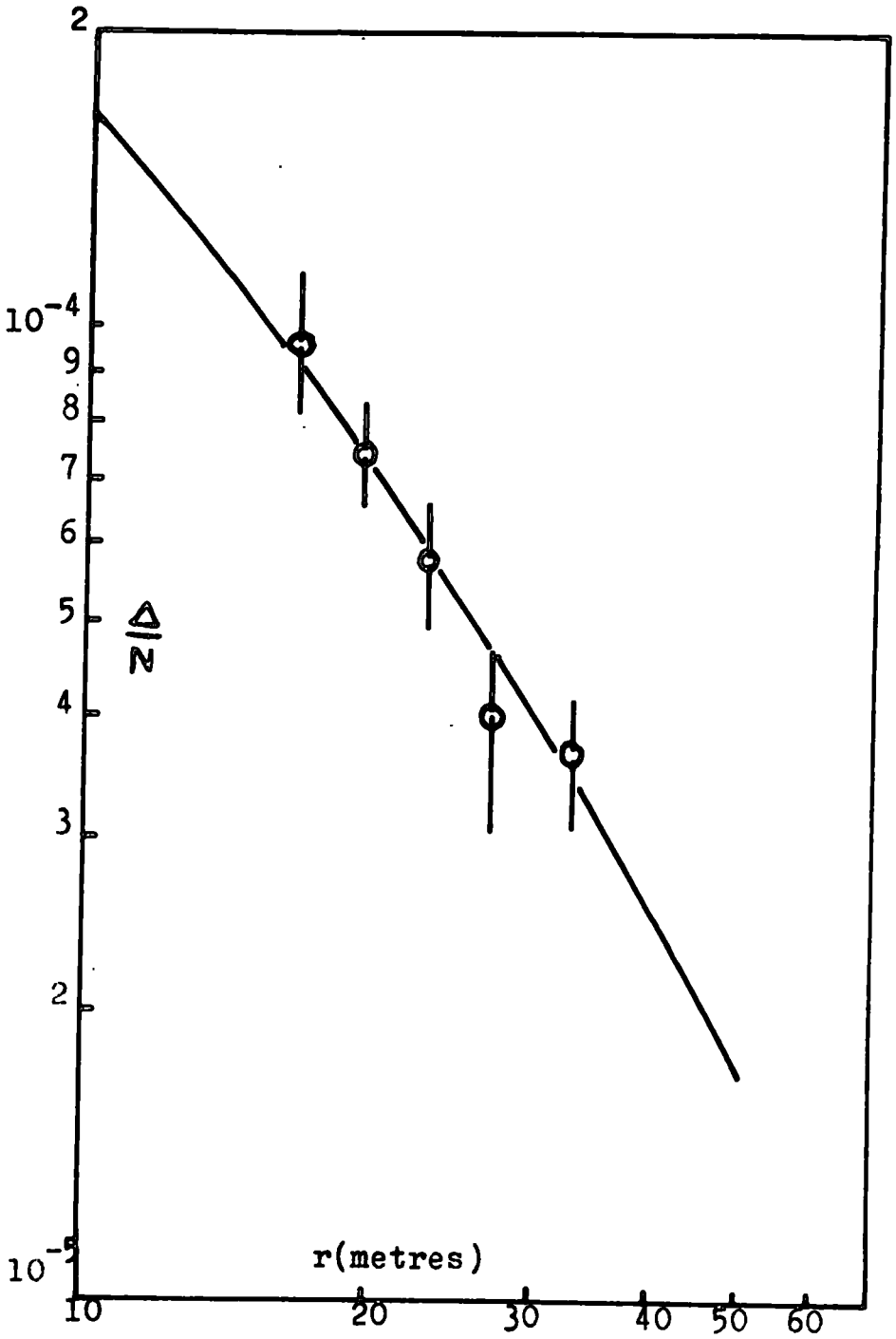

FIG.6.5. THE STRUCTURE FUNCTION.

6.5 Conclusions and Future Work

The experimental work carried out both at Durham and at Silwood Park shows that a large array of neon flash-tubes, such as D.A.S.I., is capable of precise density measurements. Previous work by Coxell (1961) using the same unit at Durham showed that accurate measurements of track directions were possible so that it can be concluded that the flash-tube technique has useful general application to studies of extensive air showers.

A possible application of the present instrument (D.A.S.I.) is to dismantle the layers and use a large collecting array for numerous estimates of the density of particles at prescribed distances from the shower axis. A total area of 16 m^2 could be presented in this way. Difficulties in the recording of events would occur with the apparatus set up in this manner, although the possibilities of using photomultipliers to record the particle densities should not be overlooked.

Another possible application of arrays of flash-tubes of the D.A.S.I. type is in the measurement of the μ-meson component in showers. An arrangement of particular usefulness would consist of several large units placed on the circumference of a circle radius ~500 metres centered about a conventional array (e.g. the Haverah Park Array). A system of this type would respond mainly to μ-mesons,

which preponderate at large distances from shower cores, and would give information on their heights of origin. Such information would contribute to solving the problem of the mass composition of the primaries responsible for the very large extensive air showers.

Acknowledgments

The author wishes to express his gratitude to Professor G.D. Rochester F.R.S. for the facilities provided for the work and for his continued interest and encouragement.

He is most grateful to his supervisor, Dr. A.W. Wolfendale, for his great help and guidance throughout the whole of this work, and to Dr. H. Coxell for much helpful advice and discussions.

He is grateful to Dr. M.A. Meyer for his assistance in the work on the Light Output of the Flash-Tubes and to Dr. M.G. Thompson for helpful comments on the manuscript of this thesis.

He is also indebted to Dr. H.R. Allan of Imperial College, London and to the staff at the field station, at Silwood Park, where the equipment was located, for their assistance most readily given.

Finally his thanks are due to the Department of Scientific and Industrial Research for an Advanced Studentship Award during the period of this work.

Appendix I.

The determination of the theoretical lower limit of the variation of intensity with angle.

The filamentary character of the discharge is disregarded and it is assumed that there is a uniform cylinder of emitting gas. Further assumptions made are that reflections and self-absorption are unimportant. The variation in intensity is then given by

$$\frac{I_\theta}{I_o} = \frac{V_\theta}{V_o}$$

Where V_o is the volume of the cylinder and V_θ is the volume visible through the circular window when viewed at angle θ. In order that this volume may be calculated it is necessary to consider the areas which are shown shaded in the diagrams for (a) very small angle θ, (b) where $\tan \theta_o = \frac{r}{l}$ and (c) for angles great than θ_o.

If $l >> r$ the areas at the centre of the tube where h = 0 are given by

$$A'B'CD' = 4rl - 2l^2 \tan \theta \qquad \text{(i)}$$

$$AB'D = 2rl \qquad \text{(ii)}$$

$$A'B'F = 2\, r^2 \cot \theta \qquad \text{(iii)}$$

As $l >> r$ it is only necessary to consider equation (iii) and disregard the small ellipticity of the front end of the tube when viewing at relatively small angles.

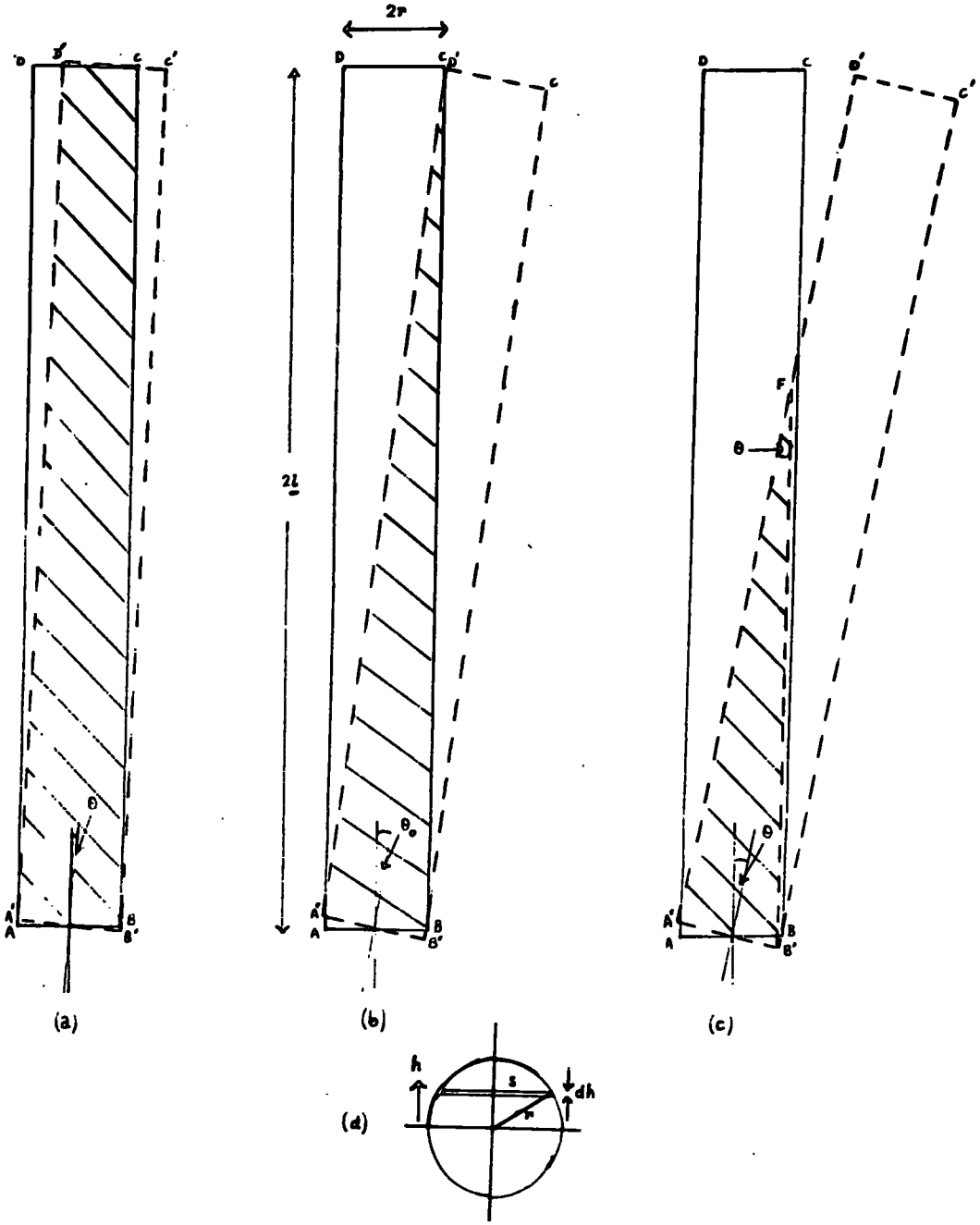
2r
2l
θ
θ₀
F
h
s
dh
r
(a)
(b)
(c)
(d)

The volume of a small element of thickness dh at a height h in the tube for angle $\theta > \theta_o$ is

$$dV_\theta = 2s^2 \cot\theta d\theta$$

from (d) $$s^2 = r^2 - h^2$$

hence $$V_\theta = 2 \cot\theta \int_{-r}^{+r} (r^2-h^2)dh$$

$$= \frac{8}{3} r^3 \cot\theta$$

and $$\frac{V_\theta}{V_o} = \frac{4}{3\pi} \left(\frac{r}{l}\right) \cot\theta \qquad \text{for } \theta > \theta_o.$$

Appendix II

Circuit Diagrams

(a) Rossi Coincidence Circuit.

(b) Pulse forming circuit.

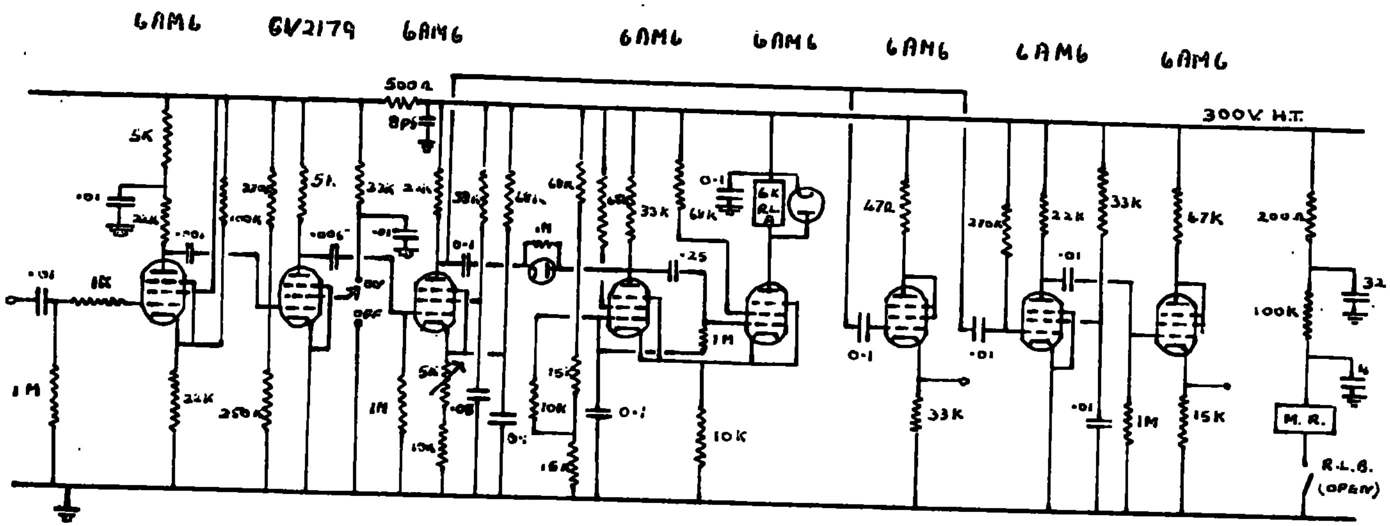

6AM6
6V2179
6AM6
6AM6
6AM6
6AM6
6AM6
6AM6
300V H.T.
500Ω
5K
1M
1K
33K
47Ω
270K
22K
67K
200Ω
100K
15K
10K
0·1
·01
·25
M. R.
R.L.B.
(OPEN)

(a)

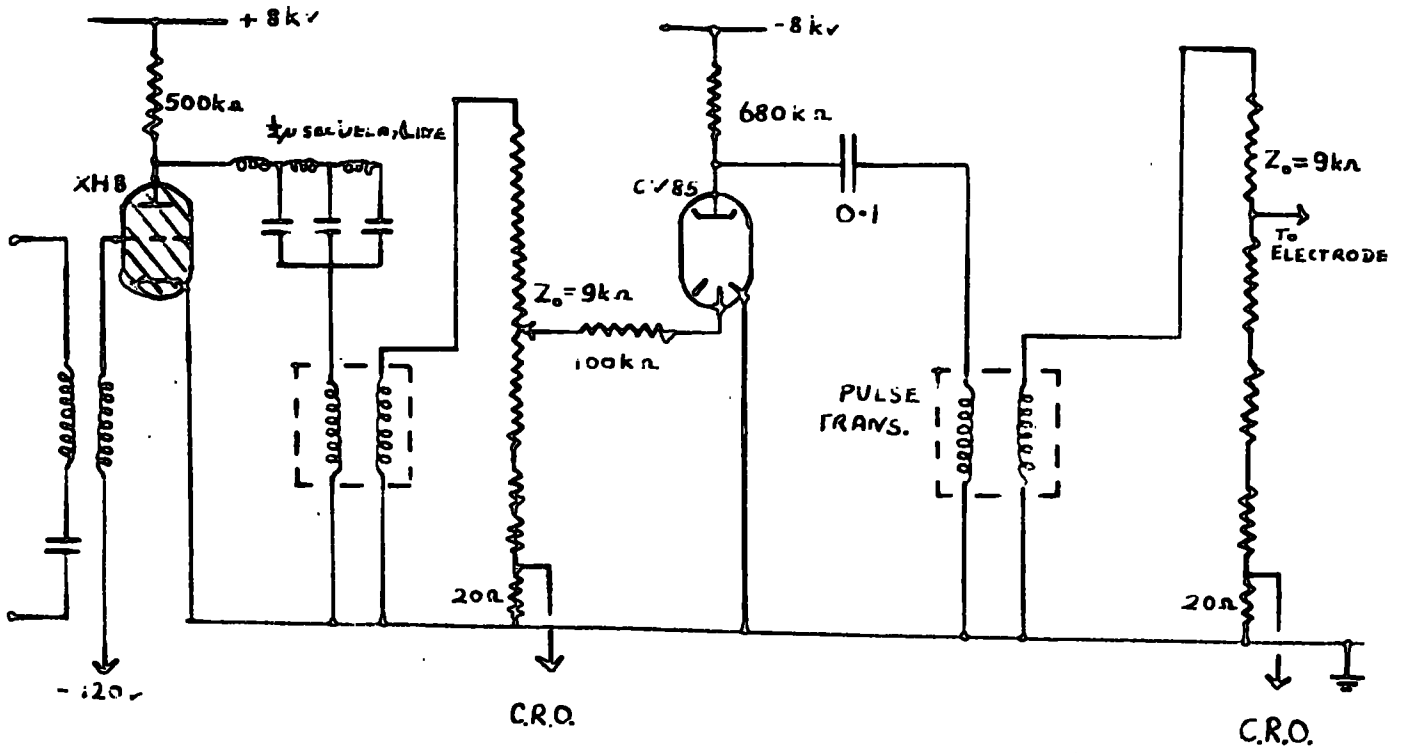
+8kv
500kΩ
½μ SECTIONS, LINE
XH8
-8kv
680kΩ
CV85
0·1
Z_o=9kΩ
100kΩ
Z_o=9kΩ
To ELECTRODE
PULSE TRANS.
20Ω
20Ω
-120v
C.R.O.
C.R.O.

(6)

References

General

Allan, H.R., 1960, Colloquium E.A.S., Imperial College, London.

Galbraith, W.,
1958, Extensive Air Showers, Butterworth Press, London.

Greisen, K., 1960, Annual Review of Nuclear Science, Vol 10.

Abrosimov, A.T., Bazilevskaya, G.A., Solovieva, V.I., and Khristiansen, G.B.,
1960, Zh.Eksp.Teor.Fiz., 38, 100 (Soviet Phys., JETP, 11, 74).

Allan, H.R., Beamish, R.F., Bryant, D.A., Kasha, H., and Wills, R.D.,
1960, Proc. Phys. Soc., 76, 1.

Allan, H.R., Beamish, R.F., Glencross, W.M., Thomson, D.M., and Wills, R.D.,
To be published, Proc. Phys. Soc.

Clark, G., Earl, J., Kraushaar, W., Linsley, J., Rossi, B., and Scherb, F.,
1958, Nuovo Cim., Suppl. 8, 10, 623.

Coxell, H., and Wolfendale, A.W.,
1960, Proc. Phys. Soc., 75, 378.

Coxell, H., 1961, Thesis Durham University.

Coxell, H., Meyer, M.A., Scull, P.S., and Wolfendale, A.W.,
1961, Nuovo Cim. Suppl. Vol. 21, Ser. X, 7.

Coxell, H., Scull, P.S., and Wolfendale, A.W.,
To be published.

Fukui, S., Hasegawa, H., Matano, T., Muira, I., Oda, M.,
Suga, K., Tanahashi, G., and Tanuka, Y.,
1960, Prog. Theor. Phys. Suppl. 16, 1.

Kamata, K., and Nishimura, J.,
1958, Prog. Theor. Phys. Suppl. 6, 93.

Kameda, T., Toyoda, Y., and Maeda, T.,
1960, J. Phys. Soc. Japan, 15, 1565.

Kulikov, G.Y., and Khristiansen, G.B.,
1958, Zh.Eksp.Teor.Fiz., 35, 635 (1959, Soviet
Phys. JETP, 8, 441).

Kulikov, G.V., Nesterova, N.M., Nikol'skii, S.I., Solovieva,
V.I., Khristiansen, G.B., and Chudakov,
A.E.,
1959, Proc. Moscow Cosmic Ray Conf. (IUPAP),
2, 85.

Norman, R.J., 1956, J. Aust. Phys. 8, 419.

Prescott, J.R.,
1956, Proc. Phys. Soc., A69, 870.

Reid, R.J., Gopaulsingh, K., Page, D.E., Idnum, M.,
McCusker, C.B.A., Malos, J., Millar,
D.D., and Winterton, G.,
1962, Proc.Int.Conf. on Cosmic Rays and Earth
Storms, Kyoto III, 234.